Published in final edited form as:
Neuroscience. 2011 December 1; 197: 251–268. doi:10.1016/j.neuroscience.2011.09.011.

Swim stress activates serotonergic and non-serotonergic neurons in specific subdivisions of the rat dorsal raphe nucleus in a temperature-dependent manner

Kyle J. Kelly[1,*], **Nina C. Donner**[1], **Matthew W. Hale**[2], and **Christopher A. Lowry**[1,3]

[1]Department of Integrative Physiology and Center for Neuroscience, University of Colorado Boulder, Boulder, CO, 80309-0354, USA

[2]School of Psychological Science, La Trobe University, Melbourne, VIC 3086, Australia

[3]Henry Wellcome Laboratories for Integrative Neuroscience and Endocrinology, University of Bristol, Bristol, UK, BS1 3NY

Abstract

Physical (exteroceptive) stimuli and emotional (interoceptive) stimuli are thought to influence stress-related physiologic and behavioral responses through different neural mechanisms. Previous studies have demonstrated that stress-induced activation of brainstem serotonergic systems is influenced by environmental factors such as temperature. In order to further investigate the effects of environmental influences on stress-induced activation of serotonergic systems, we exposed adult male Wistar rats to either home cage control conditions or a 15 min swim in water maintained at 19 °C, 25 °C, or 35 °C and conducted dual immunohistochemical staining for c-Fos, a marker of immediate-early nuclear activation, and tryptophan hydroxylase (TPH), a marker of serotonergic neurons. Changes in core body temperature were documented using biotelemetry. As expected, exposure to cold (19 °C) swim, relative to warm (35 °C) swim, increased c-Fos expression in the external lateral part of the parabrachial nucleus (LPBel), an important part of the spinoparabrachial pathway involved in sensation of cold, cutaneous stimuli, and in serotonergic neurons in the raphe pallidus nucleus (RPa), an important part of the efferent mechanisms controlling thermoregulatory warming responses. In addition, exposure to cold (19 °C) swim, relative to 35 °C swim, increased c-Fos expression in the dorsal raphe nucleus, ventrolateral part/periaqueductal gray (DRVL/VLPAG) and dorsal raphe nucleus, interfascicular part (DRI). Both of these subregions of the dorsal raphe nucleus (DR) have previously been implicated in thermoregulatory responses. Altogether, the data are consistent with the hypothesis that midbrain serotonergic neurons, possibly via activation of afferents to the DR by thermosensitive spinoparabrachial pathways, play a role in integration of physiologic and behavioral responses to interoceptive stress-related cues involved in forced swimming and exteroceptive cues related to cold ambient temperature.

[*]Corresponding author: Kyle Kelly, Department of Integrative Physiology and Center for Neuroscience, University of Colorado at Boulder, 1725 Pleasant St, Boulder, CO 80309-0354, USA, Tel: (303)-492-8154, Fax: (303)-492-0811, kyle.kelly@colorado.edu.

Conflict of Interest Statement

The authors declare that they have no conflicts of interest.

Keywords

c-Fos; dorsal raphe nucleus; lateral parabrachial nucleus; raphe pallidus; serotonin; spinoparabrachial

Environmental factors influence physiologic and behavioral responses to aversive stimuli. For example, water temperature during forced swimming has profound influences on core body temperature (Tb) that are associated with changes in behavioral stress coping responses in rats (Linthorst et al., 2008; Pinter et al., 2011). The neural mechanisms underlying the interactions between environmental factors and stress coping behaviors are not clearly understood, but may involve integration of physiologic and behavioral responses by brainstem neuromodulatory systems, including serotonergic systems. In support of this hypothesis, environmental temperature alters extracellular serotonin (5-hydroxytryptamine; 5-HT) concentrations in forebrain limbic structures controlling stress-induced emotional behavior (Linthorst et al., 2008).

It is clear that brainstem neuromodulatory systems, including serotonergic systems, play an important role in control of both emotional behavior and thermoregulatory responses. For example, serotonergic systems are thought to play an important role in proactive versus reactive emotional coping behavior (Chung et al., 1999; Chung et al., 2000; Koolhaas et al., 2007). In addition serotonergic systems are known to be involved in thermoregulation (Hedlund and Sutcliffe, 2004; Hodges and Richerson, 2010; Ray et al., 2011; Morrison and Nakamura, 2011) and therefore may be important for the integration of behavioral and thermoregulatory responses during exposure to aversive stimuli. For example, medullary serotonergic systems in the raphe pallidus nucleus (RPa) of the brainstem are thought to project to the intermediolateral column of the spinal cord, where they act on 5-HT_{2A} receptors to promote cutaneous vasoconstriction and on 5-HT_{1A} receptors to promote brown adipose tissue (BAT) thermogenesis. In contrast to the well-established role of medullary serotonergic systems in thermoregulation, it is less clear what role serotonergic systems play within the midbrain raphe complex, including the dorsal (DR) and median raphe nuclei (MnR), in the integration of cold thermosensory and efferent thermoregulatory warming responses. Several lines of evidence suggest that serotonergic neurons in the midbrain raphe complex are important for the integration of these responses. First, cells in the DR show increased c-Fos induction in response to acute cold ambient temperature (Bratincsak and Palkovits, 2004). Second, serotonergic neurons in the midbrain raphe complex are sensitive to local decreases in temperature (Cronin and Baker, 1977). Third, electrical stimulation of the DR increases BAT (Dib et al., 1994). Fourth, direct microinjection of 5-HT into the medial preoptic area (MPO) can induce a pronounced hyperthermia (Huttunen et al., 1988; Datta et al., 1988). A role for midbrain serotonergic systems in the effects of exteroceptive stimuli such as temperature on physiologic and behavioral responses to aversive stimuli is supported by findings that water temperature profoundly alters extracellular 5-HT concentrations in limbic forebrain structures during exposure to aversive stimuli (Linthorst et al., 2008). Specifically, exposure of rats to swim stress (SS) at 35 °C results in increased extracellular 5-HT and 5-HT metabolite (5-hydroxyindoleacetic acid, 5-HIAA) concentrations in the ventral hippocampus, while exposure of rats to SS at 19 °C results in delayed increases in extracellular 5-HT and 5-HIAA concentrations. The delayed 5-HT/5-HIAA increases coincide with the onset of thermoregulatory warming following exposure to SS. Also, while 5-HIAA concentrations are increased following SS at 35 °C, extracellular 5-HIAA concentrations are dramatically decreased during exposure to swimming at 19 °C suggesting that exposure to cold swim decreases mesolimbocortical serotonergic neurotransmission during SS.

The ability to thermoregulate in response to cold ambient temperature is important for survival of all endotherms. Although physiological responses to cold ambient temperature, for example cutaneous vasoconstriction, BAT thermogenesis and shivering thermogenesis, have been well characterized in rodent models (Rathner and McAllen, 1998; Golozoubova et al., 2001; Cano et al., 2003; Cannon and Nedergaard, 2004; Nason, Jr. and Mason, 2004; Golozoubova et al., 2006; Nason, Jr. and Mason, 2006), the thermoafferent pathways, and integration of afferent information to elicit physiological responses are less well understood. Recent studies have demonstrated that afferent signals from peripheral cold sensors are relayed to the brain via a spinoparabrachial pathway synapsing in the lateral parabrachial nucleus (LPB) (Bester et al., 1997; Kobayashi and Osaka, 2003; Nakamura and Morrison, 2008; Nakamura and Morrison, 2010). Glutamatergic neurons in the LPB in turn project to the MPO, where they control, via multisynaptic descending pathways, thermoregulatory warming responses, including vasoconstriction of cutaneous blood vessels, activation of BAT thermogenesis, and activation of shivering thermogenesis (Morrison and Nakamura, 2011).

Based on previous studies demonstrating that subpopulations of serotonergic neurons within the DR are thermosensitive (Hale et al., 2011), we hypothesized that a subpopulation of serotonergic neurons in the DR is cold-sensitive and therefore may mediate interactions between interoceptive and exteroceptive stimuli controlling neurochemical and behavioral responses under aversive conditions. In order to test this hypothesis, we exposed rats to a 15 min forced swim session at 19 °C, 25 °C, or 35 °C and performed dual immunohistochemical staining for c-Fos, the protein product of the immediate-early gene, *c-fos*, and tryptophan hydroxylase (TPH), a marker of serotonergic neurons. We then explored correlations between Tb, activation of the spinoparabrachial pathway, as evidenced by increases in c-Fos expression in cold-sensitive subregions of the LPB, and activation of midbrain and medullary serotonergic systems, as evidenced by increases in c-Fos expression in the DR and RPa.

1. Experimental Procedures

1.1 Animals

Adult male Wistar rats (HSD-WI, Harlan Labs, Indianapolis, IN, USA; 225–250 g) were used throughout the course of the experiment. Thirty-five experimental rats were pair housed in transparent Plexiglas® cages (26 cm W × 47.6 cm L × 20.3 cm H; Cat. No., RC88D-PC, Alternative Designs, Siloam Springs, AR, USA) using standard cage bedding (Teklad Laboratory Grade Aspen Bedding, Harlan, Madison, WI, USA). Both food (Cat No. 2018, Teklad Global 18% Protein Rodent Diet, Harlan, Madison, WI, USA) and tap water were provided *ad libitum* for the duration of the experiment. Rats were kept on a standard 12 h: 12 h light/dark cycle, with lights on 0700 h. Rats were allowed to acclimate to housing conditions for 5–9 days prior to any experimental procedures. All experiments were conducted in accordance with the *Guide for the Care and Use of Laboratory Animals*, Eighth Edition (Institute for Laboratory Animal Research, The National Academies Press, Washington, D.C., 2011) and were submitted to, and approved by, the University of Colorado Institutional Animal Care and Use Committee. All possible efforts were made to minimize the number of animals used and their suffering.

1.2 Surgical procedures

Telemetric probes were implanted into the peritoneal cavity. The surgery was performed under inhaled isoflurane anesthesia (5% initial and 2% maintenance). Briefly, following anesthesia the rat was placed onto its back, the rat's abdominal hair was shaved, and its skin was disinfected with a 10% povidone-iodine solution (Qualitest Pharmaceuticals, Huntsville,

AL, USA), and with 70% ethanol. A 1 cm midline incision was made through both the dermis and abdominal muscle wall, starting just caudal to the xiphoid process of the sternum. A telemetric probe (Model No. TAF-40; Data Sciences International (DSI), St. Paul, MN, USA) was sterilized with Actril (Cat. No. 176-02-046, Minnetech, Minneapolis, MN, USA) and implanted into the peritoneal cavity. Following probe implantation the abdominal wall was sutured using 3-0 non-absorbable silk surgical suture (Cat. No. MV-684, Med-Vet International, Mettawa, IL, USA) in a simple interrupted pattern (3 stitches). The dermal tissue was rejoined using two sterile stainless steel wound clips (Cat. No. 12032-09, Fine Science Tools Inc., Foster City, CA, USA). Antibacterial wound wash (Nolvasan, Fort Dodge Animal Health, Fort Dodge, IA, USA) was applied following suturing, and the rat was placed on a 37 °C heating pad until full recovery. Upon recovery a 5 mg/kg dose of the post-surgical analgesic carprofen (Rimadyl, Pfizer Animal Health, New York, NY, USA) was administered subcutaneously. After the surgery, all rats were single-housed in clean cages with fresh bedding. Rats were allowed to recover from surgery and acclimate for 10 days post-surgery before behavioral testing.

1.3 Experimental design

Four treatment groups were used in the experiment: a home cage control group (n = 8) that was left undisturbed and rats that were forced to swim at 19 ± 1 °C (n = 9), 25 ± 1 °C (n= 9), or 35 ± 1 °C (n = 9). All rats in this study were implanted with biotelemetry probes to measure core body temperature (°C) and motor activity (arbitrary units). Swim stress consisted of a 15 minute swim period. Two hours following the end of the swim session rats were deeply anesthetized with sodium pentobarbital (90 mg/kg; Fatal-Plus, Vortech Pharmaceutical, Dearborn, MI, USA) prior to perfusion and collection of brain tissue for immunohistochemical procedures.

Swim stress (SS)—Swim stress (SS) was performed using a Pyrex® glass cylinder (45.7 cm H × 30.5 cm diameter; Cat No. 36360-201, VWR, West Chester, PA, USA), and a water depth of 30 cm. Briefly, rats were placed into a glass cylinder filled with water of the appropriate temperature for 15 minutes and allowed to explore the environment. Following the 15 minute SS, rats were dried with a towel and placed back into their home cages. Digital video cameras (Sony Handycam Model No. DCR-HC35E and DCR-H52, Sony Corporation of America, New York, NY, USA) were used to record behavior from a horizontal viewing plane during the SS, and the rats' behaviors during the SS was scored later using a behavioral computer software (The Observer® XT, Noldus Information Technology, Wageningen, The Netherlands). Briefly, the rat's behavior during SS was categorized into 'swimming', 'climbing', and 'immobility', using continuous sampling. Swimming was defined as any movement across the water surface that was more than necessary for the rat to keep its head above water. Climbing was defined as upward movement directed to the sides of the forced swim chamber, with the front paws breaking the water surface. Immobility was defined as lack of activity other than that required to maintain the rat's head above water (Detke et al., 1995). Dives (submersion of the rat's entire body) were classified as instantaneous events outside of the ongoing continuous sampling. The scorer was blind to the treatment groups.

1.4 Biotelemetry

Three rats at a time were exposed to SS (19 °C, 25 °C, and 35 °C), while a fourth rat remained in its home cage (HC control group). Core body temperature (C) and motor activity (recorded as arbitrary units) were monitored continuously at a frequency of 128 Hz during five-second samples in one-minute intervals. Recording began 125 min prior to the onset of the 15-min long SS, and continued for 2 h after termination of SS. Telemetric receivers (DSI Physiotel® Receiver, Model No. RPC-1) placed below the rat's home cage

transmitted signals to a computer before and after the SS session. During the SS session, Tb was recorded with the receivers placed below the forced swim cylinder. Telemetric signals were processed and recorded using the software 'Dataquest ART' (version 3.0, DSI).

1.5 Tissue fixation and sectioning

Following the induction of anesthesia, rats were transcardially perfused with ice-cold 0.05 M phosphate-buffered saline (PBS, pH 7.4) followed by an ice-cold 4% paraformaldehyde solution (prepared using 80 g paraformaldehyde, 30 g sucrose, 4.8 mL sodium hydroxide, 808 ml 0.2 M $Na_2HPO_4{\cdot}7H_2O$, 192 ml $NaH_2PO_4{\cdot}H_2O$, 1 L distilled H_2O (dH_2O)). Following fixation, the brains were removed and post-fixed in 4% paraformaldehyde solution for 24 h at 4 °C and were then rinsed in 0.1 M sodium phosphate buffer (PB; 80.8% 0.1 M $Na_2HPO_4{\cdot}7H_2O$ and 19.2% 0.1 M $NaH_2PO_4{\cdot}H_2O$) twice for 12 h each. The brains were then placed in 30% sucrose in 0.1 M PB until they had sunk, dissected into forebrain and hindbrain with a cut in the coronal plane at the caudal border of the mammillary bodies (approximately −5.80 mm bregma) using a rat brain matrix (RBM-4000C, ASI Instruments, Warren, MI, USA) to ensure a consistent coronal plane of sectioning, rapidly frozen in isopentane chilled on dry ice, and then stored at −80 °C. The hindbrains were sectioned (30 μm) using a cryostat (Leica CM1900, North Central Instruments, Denver, CO, USA) and stored in cryoprotectant (prepared using 270 ml ethylene glycol, 160 ml glycerol, 202 ml 0.2 M $Na_2HPO_4{\cdot}7H_2O$, 48 ml 0.2 M $NaH_2PO_4{\cdot}H_2O$, and 320 ml dH_2O) at −20 °C as 6 alternate sets of sections until immunohistochemical procedures were conducted.

1.6 Antibodies

For immunodetection of tryptophan hydroxylase (TPH), an affinity-isolated antibody (sheep anti-TPH antiserum, Cat. No. T8575, Lot No, 047K1223, Sigma-Aldrich, St. Louis, MO, USA), raised against recombinant rabbit TPH was used. Briefly, the antibody was isolated as inclusions bodies from *Escherichia coli* and purified by preparative sodium dodecyl sulfate polyacrylamide gel electrophoresis (SDS-PAGE), as immunogen was used. This antibody has been characterized previously, and has been shown to bind both TPH1 and TPH2 isoforms (Hale et al., 2011). For immunodetection of the protein product of the immediate-early gene *c-fos*, an affinity-isolated antiserum (rabbit anti-c-Fos polyclonal antibody, Cat. No. PC38 (Ab-5), Lot No. 88552, 1:3000; EMD Biosciences, San Diego, CA, USA), raised against a synthetic peptide (SGFNADYEASSSRC) corresponding to amino acids 4–17 of human c-Fos protein was used. This antibody has previously been characterized and has been shown to bind specifically to amino acids 4–17 of the human c-Fos protein (Rinaman et al., 1997).

1.7 Immunohistochemistry

Immunohistochemistry for c-Fos and TPH was conducted on free-floating tissue in 12-well tissue culture plates in 1.5 mL of solution and gently shaken on an orbital shaker throughout the staining process. Unless stated otherwise, tissue was washed for 15 min. Tissue was rinsed twice in 0.05 M phosphate buffered saline (PBS) followed by washing in 0.05 M PBS containing 1% hydrogen peroxide (H_2O_2). Tissue was then was rinsed twice in 0.05 M PBS followed by one wash in 0.05 M PBS containing 0.1% Triton X-100 and 0.01% sodium azide (NaN_3) (0.1% PBST + 0.01% NaN_3). Sections were then incubated overnight at room temperature with 1:3000 rabbit anti-c-Fos polyclonal antibody in 0.1% PBST + 0.01% NaN_3. After 16 hours, tissue was washed twice in 0.05 M PBS followed by incubation with 1:200 biotinylated donkey anti-rabbit IgG (Cat. No. 711-065-152, Lot No. 89828, Jackson Immunolabs, West Grove, PA, USA) in 0.05 M PBS for 90 min. Tissue was then washed twice in 0.05 M PBS followed by incubation with an avidin-biotin peroxidase complex (Elite ABC reagent, Cat. No. PK-6100, 1:200; Vector Laboratories, Burlingame, CA, USA) in 0.05 M PBS for 90 min. Tissue was washed twice in 0.05 M PBS then placed in a

peroxidase substrate solution (SG substrate, Cat. No. SK4700, Vector Laboratories, diluted as recommended by the vendor) in 0.05 M PBS for 10 min. Immediately after the chromogen reaction, sections were washed twice in 0.05 M PBS followed by one wash in 1% H_2O_2 in 0.05 M PBS. Tissue was then washed twice in 0.05 M PBS followed by an overnight incubation in sheep anti-TPH in 0.1% PBST+ 0.01% NaN_3. After 16–20 hours, tissue was washed twice in 0.05 M PBS followed by a 90-min incubation in biotinylated rabbit anti-sheep IgG (Vectastain Elite, Cat. No. PK-6016, 1:200; Vector Laboratories) in 0.05 M PBS. After incubation, tissue was washed twice in 0.05 M PBS followed by incubation with an avidin-biotin peroxidase complex (Elite ABC reagent; Cat. No. 6100, 1:200; Vector Laboratories) in 0.05 M PBS for 90 min. Tissue was washed twice in 0.05 M PBS followed by an 18 minute incubation in 0.01% 3–3′-diaminobenzidine tetrahydrochloride (DAB, Cat. No. D9015, Sigma-Aldrich) in 0.05 M PBS with 0.0066% H_2O_2. Immediately following the chromogen reaction tissue was rinsed twice in 0.05 M PBS to stop the reaction. Brain sections were stored in 0.1 M PB with 0.01% NaN_3 at 4 °C until tissue mounting. Lastly, brain sections were rinsed in 0.1 M PB and then in 0.15% gelatin in dH_2O, before being mounted on glass microscope slides (VistaVision UniMark microscope slides, Cat. No. 16005-106; VWR Scientific, West Chester, PA, USA), dehydrated through an ascending alcohol series and cleared with xylene. Sections were preserved with cover slips and mounting medium (Entellan; Cat. No. RT14082, EM Sciences, Hatfield, PA, USA).

1.8 Cell counting

1.8.1 Dorsal raphe nucleus (DR)—Five rostrocaudal levels of the DR were chosen for analysis (−7.46, −8.00, −8.18, −8.54, and −8.72 mm bregma; Figure 1). The subdivisions of the DR studied included the dorsal raphe nucleus, dorsal part (DRD) and dorsal raphe nucleus, ventral part (DRV) at −7.46 mm bregma, the DRD, DRV, and dorsal raphe nucleus, ventrolateral part/ventrolateral periaqueductal gray (DRVL/VLPAG) at −8.00 mm bregma, the DRD, DRV, DRVL/VLPAG, and dorsal raphe nucleus, interfasicular part (DRI) at −8.18 mm bregma, the DRI and dorsal raphe nucleus, caudal part (DRC) at −8.54 mm bregma, and the DRI and DRC at −8.72 mm bregma. Rostrocaudal levels and anatomical divisions of the midbrain raphe complex were based on comparison of immunostained sections to a stereotaxic rat brain atlas (Paxinos and Watson, 1998), and an atlas of TPH immunostaining in the rat DR (Abrams et al., 2004). Cell counting of c-Fos-immunoreactive (ir)/TPH-ir, c-Fos-ir/TPH-immunonegative (−), and total TPH-ir neurons was performed. Cells were counted from both left and right sides of the DRVL/VLPAG and summed to give a total number of cells. In a limited number of cases (N = 9 out of 70 sections) from all rats at all rostrocaudal levels sampled where one side of the DRVL/VLPAG was damaged, unilateral counts were doubled for use in statistical analysis and graphical representations of the data. All remaining cell counts were from midline subdivisions. Cell counts were performed under brightfield microscopy at a total magnification of 100x. If necessary, a total magnification of 400x was used to verify double immunostaining. The experimenter was blind to the treatment groups throughout cell counting.

1.8.2 Lateral parabrachial nucleus (LPB)—Three rostrocaudal levels of the LPB were chosen for analysis (−9.16, −9.34, and −9.70 mm bregma; Figure 2), based on previous studies of thermosensitive neurons in the LPB (Nakamura and Morrison, 2010). The subdivisions of the LPB studied include the LPB, external lateral part, (LPBel) and LPB, dorsal part (LPBd) at −9.16 mm bregma, the LPBel, and LPBd at −9.34 mm bregma, and the LPBel at −9.70 mm bregma. Rostrocaudal levels and anatomical divisions of the LPB were based on comparison of immunostained sections to a stereotaxic rat brain atlas (Paxinos and Watson, 1998). Cell counting of c-Fos-ir cells was performed using grid analysis. Grid sizes were 0.4 mm × 0.2 mm for the LPBel and LPBd at −9.16 mm bregma,

0.4 mm × 0.2 mm for the LPBel and 0.5 mm × 0.2 mm for the LPBd at −9.34 mm bregma, and 0.4 mm × 0.2 mm for the LPBel at −9.70 mm bregma (Figure 2). Cells were counted from both left and right sides of the LPBel and LPBd and summed to give a total number of cells. In a limited number of cases (N = 26 sections, 15.3% of total data for the LPB) where one side of the LPB was damaged, unilateral counts were doubled for use in statistical analysis and graphical representations of the data. Cell counts were performed under brightfield microscopy at a total magnification of 100x. The experimenter was blind to the treatment groups throughout cell counting.

1.8.3 Raphe pallidus nucleus (RPa)—Three rostrocaudal levels of the RPa were chosen for analysis: −11.24, −11.60, and −11.78 mm bregma (Figure 3). Rostrocaudal levels of the RPa were based on comparison of immunostained sections to a stereotaxic rat brain atlas (Paxinos and Watson, 1998). Cell counting of c-Fos-ir/TPH-ir, c-Fos-ir/TPH–, and total TPH-ir neurons was performed. Cell counts were performed under brightfield microscopy at a total magnification of 100x. If necessary, a total magnification of 400x was used to verify double immunostaining. The experimenter was blind to the treatment groups throughout cell counting.

1.9 Image capture

Representative photomicrographs were taken using a Nikon 90i microscope and a Nikon DS-Fi1 digital camera linked to a computer with NIS Elements 3.00 imaging software (A.G. Heinze Inc., Lake Forest, CA, USA).

1.10 Statistical analysis

All statistical analyses were performed using PASW statistics (Version 18 for Windows, SPSS Inc., Chicago, IL, USA). Data in figures are presented as group means + SEMs. Statistical significance is denoted in the graphs.

1.10.1 Swim stress data—A one-way analysis of variance (ANOVA) with *water temperature* as a between-subjects factor was used to determine the effect of water temperature on swimming, immobility, climbing, and diving behaviors during SS. Grubbs test (Grubbs, 1969) was used to identify any outliers (N = 2, 1.85% of the total dataset; 1 outlier immobility (35 °C), 1 outlier climbing (19 °C)) and outliers were removed. When appropriate, Fisher's Protected Least Significant Difference (LSD) tests were used for post hoc comparisons. Statistical significance was accepted at the level of $p < 0.05$ for both the ANOVA and post hoc comparisons.

1.10.2 Telemetric data—A multifactor ANOVA with repeated measures was used to analyze telemetric data for Tb (°C), expressed as the average temperature in 5 minute time bins. Core body temperature was analyzed using *treatment* (four levels: Home cage (HC), 19 °C, 25 °C, and 35 °C SS) as a between-subjects factor and *time* (52 levels) as a within-subjects factor for the repeated measures analysis. A Greenhouse-Geisser epsilon correction (ε) was used for repeated measures to correct for violation of the sphericity assumption. Grubbs test was used to identify and remove any outliers (temperature, N = 435, 3.10%). Replacement data for missing data (temperature, N = 435, 3.10%) for the multifactor ANOVA with repeated measures were calculated using the Petersen method (Petersen, 1985). Replacement data were not used in graphical representations of the data or in planned pairwise comparisons. Significance was accepted at the level of $p < 0.05$. If significance was reached in the multifactor ANOVA with repeated measures, Bonferroni tests were used for planned pairwise comparisons.

1.10.3 Cell count data—Cell counts within the DR for the numbers of c-Fos-ir/TPH-ir (serotonergic) neurons, the numbers of c-Fos-ir/TPH– (non-serotonergic) cells and the total numbers of TPH-ir neurons sampled were analyzed separately using a multifactor ANOVA with repeated measures using *treatment* (four levels: Home Cage (HC), 19 °C, 25 °C, and 35 °C SS) as a between-subjects factor and *brain region* (13 levels) as a within-subjects factor for the repeated measures analysis. A Greenhouse-Geisser epsilon correction (ε) was used for repeated measures to correct for violation of the sphericity assumption. Grubbs test was used to identify outliers (c-Fos-ir/TPH-ir neurons, N = 1, 0.19%; c-Fos-ir/TPH– cells, N = 3, 0.57%; total TPH-ir neurons, N = 2, 0.38%) and outliers were removed. Replacement values for missing data (c-Fos-ir/TPH-ir neurons, N = 25, 4.76%; c-Fos-ir/TPH– cells, N = 25, 4.76%; total TPH-ir neurons, N = 26, 4.95%) for the multifactor ANOVA with repeated measures were calculated using the Petersen method (Petersen, 1985). Replacement data were not used in graphical representations of the data or in planned pairwise comparisons. Significance was accepted at the level of $p < 0.05$. If significance was reached in the multifactor ANOVA with repeated measures, Fisher's Protected LSD tests were used for planned pairwise comparisons.

Cell counts within the LPB for the number of c-Fos-ir cells were analyzed using an analysis of variance (ANOVA) with *treatment* (four levels: HC, 19 °C, 25 °C, and 35 °C SS) as a between-subjects factor and *brain region* (5 levels) as a within-subjects factor for the repeated measures analysis. A Greenhouse-Geisser epsilon correction (ε) was used for repeated measures to correct for violation of the sphericity assumption. Grubbs test was used to identify outliers (N = 3, 0.98% of the total data set) and outliers were removed. Replacement data (N = 11, 6.47% of the total data set) for the multifactor ANOVA with repeated measures was calculated using the Petersen method. Replacement data were not used in graphical representations of the data or in planned pairwise comparisons. Significance was accepted at the level of $p < 0.05$. If significance was reached in the multifactor ANOVA with repeated measures, Fisher's Protected LSD tests were used for planned pairwise comparisons.

Cell counts within the RPa for the numbers of c-Fos-ir/TPH-ir (serotonergic) neurons, the numbers of c-Fos-ir/TPH– (non-serotonergic) cells and the total numbers of TPH-ir neurons sampled were analyzed using methods similar to those used for analysis of cell counts in the DR except that *brain region* only had 3 levels, outliers (c-Fos-ir/TPH-ir neurons, N = 1, 0.95%; c-Fos-ir/TPH– cells, N = 1, 0.95%; total TPH-ir neurons, N = 0) and replacement values (c-Fos-ir/TPH-ir neurons, N = 8, 7.62%; c-Fos-ir/TPH– cells, N = 8, 7.62%; total TPH-ir neurons, N = 8, 7.62%).

1.10.4 Correlations—The average numbers of c-Fos-ir serotonergic neurons from each rat, based on cell counts from all sampled rostrocaudal levels of the DRVL/VLPAG, DRI and RPa, and the average numbers of c-Fos-ir cells from each rat, based on cell counts from all rostrocaudal levels of the LPBel, were used for correlations with each other and with ΔTb. All Tb recordings before SS (120 minutes) were averaged for each rat to create a baseline value. All Tb recordings during SS (15 minutes) were averaged for each rat during the SS. For ΔTb, the absolute value of the difference between baseline Tb and average Tb during SS for each rat was used. Correlation analyses were performed on these data using Pearson's correlation.

2. Results

2.1 Swim stress behavior

Water temperature altered specific behaviors during the SS test, including immobility ($F_{(2,24)} = 19.30$, $p < 0.001$), swimming ($F_{(2,24)} = 14.18$, $p = 0.001$) and total number of dives

($F_{(2,24)}$ = 11.83, p = 0.001) but did not affect climbing behavior. Rats in 19 °C water spent more time immobile when compared to rats exposed to 25 °C or 35 °C water (Figure 4A). In addition, rats in 19 °C water spent less time swimming when compared to rats exposed to 25 °C or 35 °C water, and rats in 35 °C water dove more frequently than rats exposed to either 19 °C or 25 °C water (Figure 4A and B).

2.3 Core body temperature

The mean pre-swim (−120 to 0 min) baseline TbS were 37.6 °C ± 0.1, 37.6 °C ± 0.1, 37.6 °C ± 0.1, and 37.7 °C ± 0.1 in HC, 19 °C, 25 °C, and 35 °C swim groups, respectively. Swim stress at 19 °C, 25 °C and 35 °C decreased Tb (as measured via biotelemetry) throughout the test (*treatment* × *time point interaction*: $F_{(153,1581)}$ = 150.80, p < 0.001, ε = 0.066). Swim stress at different water temperatures differentially affected Tb relative to the HC control condition (Figure 5). Swim stress exposure at 19 °C, relative to HC controls, decreased Tb from 0 to 70 minutes (p < 0.001 from 0–65 minutes, p < 0.01 at 70 minutes) and increased Tb from 90 to 130 minutes (p < 0.05 at 90 minutes; p < 0.01 at 95 minutes; p < 0.001 from 100–120 minutes; p < 0.01 from 125–130 minutes) after the onset of swim stress. Swim stress exposure at 25 °C, relative to HC controls, resulted in decreased Tb from 0 to 55 minutes (p < 0.001 0–50 minutes and p < 0.05 55 minutes) and increased Tb from 90 to 100 minutes (p < 0.05 at 90 and 100 minutes; p < 0.01 at 95 minutes) after the onset of swim stress. Swim stress exposure at 35 °C, relative to HC controls, resulted in decreased Tb from 5 to 20 minutes (p < 0.05 at 5 minutes and p < 0.01 from 10–20 minutes) after the onset of swim stress.

In addition, swim stress at colder temperatures resulted in greater decreases in Tb relative to warmer temperatures. Swim stress exposure at 19 °C, relative to 25 °C, decreased Tb from 0 to 75 minutes (p < 0.001 from 0–65 minutes, p < 0.01 at 70 minutes, and p < 0.05 at 75 minutes) and increased Tb from 110 to 130 minutes (p < 0.01 from 110–115 minutes; p < 0.001 at 120 minutes, and p < 0.05 from 125–130 minutes) after the onset of swim stress. Swim stress exposure at 19 °C, relative to 35 °C, decreased Tb from 0 to 75 minutes (p < 0.001 from 0–65 minutes, p < 0.01 at 70 minutes, and p < 0.05 at 75 minutes) and increased Tb from 95 to 130 minutes (p < 0.05 at 95 minutes; p < 0.01 from 100–105 minutes; p < 0.001 from 110–115 minutes, and p < 0.01 from 120–130 minutes) after the onset of swim stress. Swim stress exposure at 25 °C, relative to 35 °C, resulted in decreased Tb from 0 to 55 minutes (p < 0.001 from 0–50 minutes and p < 0.01 at 55 minutes) after the onset of swim stress. Home cage control rats only displayed small fluctuations in Tb throughout the experiment (Figure 4C)

2.4 Immunohistochemistry

2.4.1 c-Fos-ir/TPH-ir neurons in the DR—Exposure to SS increased c-Fos-ir/TPH-ir (serotonergic) neurons in subdivisions of the DR (*treatment* × *brain region* interaction: $F_{(36,372)}$ = 1.78, p = 0.032, ε = 0.482). Exposure to SS at 19 °C, relative to home cage control conditions, increased c-Fos expression in serotonergic neurons in all subdivisions sampled except the DRI at −8.54 mm bregma (Figures 5, 6). Exposure to SS at 25 °C, relative to home cage control conditions, increased c-Fos expression in serotonergic neurons in multiple subdivisions of the DR, including the DRV and DRD at −8.00 and −8.18 mm bregma, the DRC at −8.54 and −8.72 mm bregma, and the DRI at −8.72 mm bregma (Figures 5,6). In contrast, exposure to SS at 25 °C had no effect in the rostral DR (DRV and DRD at −7.46 mm bregma), or the DRVL/VLPAG (−8.00 and −8.18 mm bregma). The effects of SS at 25 °C on c-Fos expression in serotonergic neurons in the DRI were inconsistent, with increases at −8.72 mm bregma, as mentioned above, but not at two other rostrocaudal levels (−8.18, −8.54 mm bregma). The effects of SS at 35 °C were the same as the effects of SS at 25 °C, with the exception that SS at 35 °C increased c-Fos expression in

serotonergic neurons in the rostral DR (both the DRV and DRD at −7.46 mm bregma), and had no effect at any level of the DRI studied. Swim stress at 19 °C resulted in a greater increase in c-Fos expression in serotonergic neurons, relative to SS at 25 °C in the DRVL/VLPAG (−8.18 mm bregma; this effect approached significance at −8.00 mm bregma (p = 0.085). Swim stress at 19 °C also resulted in a greater increase in c-Fos expression in serotonergic neurons relative to SS at 35 °C in the DRI (−8.18 mm bregma).

2.4.2 c-Fos-ir non-serotonergic cells in subdivisions of the DR—Exposure to SS increased c-Fos immunostaining in non-serotonergic cells in subdivisions of the DR (*treatment* × *brain region* interaction: $F_{(36,372)} = 3.73$, $p < 0.001$, $\varepsilon = 0.435$; Table 1). Exposure to SS at 19 °C, 25 °C or 35 °C relative to home cage control conditions, increased c-Fos expression in all subdivisions of the DR that were sampled. Swim stress at 19 °C resulted in a greater increase in c-Fos expression relative to SS at 25 °C in the DRV (7.46, −8.18 mm bregma), DRVL/VLPAG (−8.00, −8.18 mm bregma), and the DRI (−8.18 mm bregma). Swim stress at 19 °C resulted in greater c-Fos expression, relative to SS at 35 °C in the DRV (−7.46 mm bregma), DRVL/VLPAG (−8.18 mm bregma), and DRI (−8.18, −8.72 mm bregma). Swim stress exposure at 35 °C resulted in greater c-Fos expression, relative to 25 °C in the DRV (−8.18 mm bregma). Exposure to SS at 25 °C resulted in greater c-Fos expression, relative to 35 °C, in the DRI (−8.72 mm bregma).

2.4.3 TPH-ir neurons in subdivisions of the DR—Swim stress had no effect on the number of TPH-ir neurons in subregions of the DR (*treatment* × *brain region* interaction: $F_{(36,372)} = 0.73$, $p = 0.766$, $\varepsilon = 0.469$; *treatment*: $F_{(3,31)} = 0.35$, $p = 0.789$; Figure 6). As expected, different subregions of the DR had different numbers of TPH-ir neurons, independent of treatment (*brain region*: $F_{(12,372)} = 349.93$, $p < 0.001$, $\varepsilon = 0.469$).

2.4.4 c-Fos-ir cells in the LPB—Exposure to SS increased the numbers of c-Fos-immunostained cells in subdivisions of the LPB (*treatment* × *brain region*: $F_{(12,120)} = 6.29$, $p < 0.001$, $\varepsilon = 0.783$; Figure 7). Exposure to SS at 19 °C and 25 °C increased c-Fos expression, relative to home cage controls, in all subdivisions of the LPB studied, excluding the LPBd at −9.34 mm bregma, where neither exposure to SS at 19 °C nor 25 °C had any effect (Figure 7). In contrast, SS exposure at 35 °C differed from SS exposure at 19 °C and 25 °C, with increases in c-Fos expression, relative to home cage controls, found only in the LPBel (−9.16 and −9.70 mm bregma). Swim stress at 19 °C resulted in a greater increase in c-Fos expression relative to SS at 35 °C in the LPBel (−9.16 and −9.34 mm bregma) and the LPBd (−9.16 mm bregma). Swim stress at 25 °C resulted in a greater increase in c-Fos expression relative to SS at 35 °C in the LPBel and the LPBd (both at −9.16 mm bregma).

2.4.5 Immunohistochemistry for c-Fos and TPH in the RPa—Exposure to SS increased numbers of c-Fos-ir/TPH-ir neurons in the RPa (*treatment*: $F_{(3,31)} = 7.43$, p = 0.001; Figure 8A). Exposure to SS at 19 °C increased c-Fos expression in serotonergic neurons, relative to home cage controls, at all three levels of the RPa studied (−11.24, −11.60, and −11.78 mm bregma). Swim stress exposure at 25 °C had no effect on c-Fos expression in serotonergic neurons of the RPa relative to home cage controls. Exposure to SS at 35 °C increased c-Fos expression in serotonergic neurons, relative to home cage controls, within the rostral and caudal parts of the RPa (−11.24 and −11.78 mm bregma). Exposure to SS at 19 °C resulted in a greater increase in c-Fos expression in serotonergic neurons, relative to SS exposure at 25 °C or 35 °C, in the RPa at −11.60 mm bregma.

2.4.6 c-Fos-ir non-serotonergic cells in the RPa—Exposure to SS increased c-Fos expression in non-serotonergic cells in the RPa (*treatment* × *level*: $F_{(6,62)} = 2.87$, $p = 0.018$, $\varepsilon = 0.932$; Figure 8B). Exposure to SS at 19 °C increased c-Fos expression, relative to home

cage controls, at all rostrocaudal levels of the RPa that were sampled (−11.24, −11.60, and −11.78 mm bregma). Swim stress exposure at 25 °C increased c-Fos expression, relative to home cage controls, in the RPa at −11.60 mm bregma. Exposure to SS at 35 °C did not increase c-Fos expression relative to home cage controls. Exposure to SS at 19 °C resulted in greater c-Fos expression, relative to groups exposed to SS at 25 °C or 35 °C, at all levels of the RPa analyzed.

2.4.7 TPH-ir neurons in the RPa—Swim stress had no effect on the numbers of TPH-ir neurons in the different rostro-caudal levels of the RPa studied (*treatment* × *level* interaction: $F_{(6,62)} = 1.42$, $p = 0.224$, $\varepsilon = 0.943$; *treatment*: $F_{(3,31)} = 0.54$, $p = 0.660$; Figure 8A). As expected different rostrocaudal levels of the RPa had different numbers of TPH-ir neurons, independent of treatment (*level*: $F_{(2,62)} = 112.69$, $p < 0.001$, $\varepsilon = 0.943$).

2.5 Correlations

The ΔTb predicted the numbers of c-Fos-ir neurons in the LPB, and the numbers of c-Fos-ir serotonergic neurons in the DRVL/VLPAG, DRI, and RPa. The ΔTb during SS was positively correlated with the numbers of c-Fos-ir cells in the LPBel (r = 0.679, $p < 0.001$) (Figure 9A). The ΔTb during SS was also positively correlated with numbers of c-Fos-ir serotonergic neurons in the DRVL/VLPAG (r = 0.406, $p = 0.017$; Figure 9B), the DRI (r = 0.397, $p = 0.018$; Figure 9C), and the RPa (r = 0.382, $p = 0.024$; Figure 9D).

The numbers of c-Fos-ir cells in the LPBel predicted the numbers of c-Fos-ir serotonergic neurons in the DRVL/VLPAG, DRI, and RPa, consistent with the hypothesis that the spinoparabrachial pathway contributes to activation of brainstem serotonergic neurons following exposure to SS at different temperatures. The numbers of c-Fos-ir cells in the LPBel were positively correlated with the numbers of c-Fos-ir serotonergic neurons in the RPa (r = 0.474, $P = 0.005$; Fig. 10A), the DRVL/VLPAG (r = 0.373, $P = 0.033$; Fig 10B), and the DRI (r = 0.374, $P = 0.029$; Fig 10C).

The numbers of c-Fos-ir serotonergic neurons in the DRVL/VLPAG predicted the numbers of c-Fos-ir serotonergic and non-serotonergic neurons in the RPa. The numbers of c-Fos-ir serotonergic neurons in the DRVL/VLPAG and the DRI were positively correlated with the numbers of non-serotonergic c-Fos-ir cells in the RPa (r = 0.483, $p = 0.004$; Figure 10D) and (r = 0.594, $p < 0.001$; Figure 10E), and with the numbers c-Fos-ir serotonergic neurons in the RPa (r = 0.357, $p = 0.038$; Figure 10F).

The numbers of c-Fos-ir serotonergic neurons in subregions of the DR (DRV, DRD, DRVL, DRI, DRC) were not found to predict any of the following behaviors: diving, immobility, or swimming (data not shown). In contrast, the numbers of c-Fos-ir non-serotonergic cells in the DRV and DRD were found to predict the total immobility time (DRV, r = 0.469, $p = 0.016$; DRD, r = 0.396, $p = 0.045$). The numbers of c-Fos-ir non-serotonergic cells in the DRV were found to predict the total swim time (r = 0.452, $p = 0.018$). No other significant correlations were found between the numbers of c-Fos-ir non-sertotonergic cells in the DR and behavior.

Discussion

In these studies, we provide evidence for subpopulations of serotonergic neurons in the DR and RPa that are differentially activated following exposure of rats to cold versus warm water swim. These subpopulations are likely to be involved in the interaction of exteroceptive and interoceptive factors influencing stress-related physiology and behavior. Exposure of rats to a 15 min SS at 19 °C, 25 °C, or 35 °C decreased Tb, with the greatest decreases in Tb in the 19 °C group. Exposure of rats to SS increased c-Fos expression in

both serotonergic and non-serotonergic neurons in multiple subdivisions of the DR, regardless of the temperature; however, SS at 19 °C, which led to increased immobility during SS, resulted in a greater increase in c-Fos expression in serotonergic neurons, relative to either 25 °C or 35 °C, in two subregions of the DR that have previously been shown to be thermosensitive, the DRVL/VLPAG and DRI. ΔTb values during SS were correlated with c-Fos expression in a putative thermosensitive spinoparabrachial-raphe circuit, including the LPBel and serotonergic neurons in the DRVL/VLPAG, DRI, and RPa. Activation of the spinoparabrachial pathway, as evidenced by increased c-Fos expression in the LPBel, was correlated with activation of serotonergic neurons in the DRVL/VLPAG and DRI; activation of serotonergic neurons in the DRVL/VLPAG was in turn correlated with increased c-Fos expression in serotonergic and non-serotonergic cells within the RPa, an important part of the efferent thermoregulatory pathways controlling vasoconstriction in cutaneous vascular beds of the paws and tail, BAT thermogenesis and shivering thermogenesis.

Swim stress at 35 °C, 25 °C, and 19 °C resulted in temperature-dependent decreases in Tb. Maximal average decreases in Tb were observed at the end of the 15 min swim period; recovery to baseline Tb took considerably longer following exposure to colder temperatures, from approximately 37 ± 4.1 min in rats exposed to 35 °C, to 64 ± 3.0 min and 71 ± 2.7 min in rats exposed to 25 °C, and 19 °C, respectively. A slight overshoot in Tb was observed in rats exposed to 19 °C, with temperature rising to a maximum of 0.9 ± 0.2 °C above baseline between 73 min to 2 h following the SS. The mean minimum Tb in response to each swim condition was almost identical to that observed in a previous study (Linthorst et al., 2008). The mean minimum Tb of approximately 30 °C in response to SS at 25 °C is also similar to that observed following exposure of rats to an 80 minute intermittent cold SS paradigm using a temperature of 20 °C (Drugan et al., 2005). In contrast, exposure of rats to cold ambient temperature (4 °C for 120 min) results in relatively insignificant changes in rectal temperature, but dramatic decreases in skin surface temperature (reaching approximately 25 °C) (Bratincsak and Palkovits, 2005). Although we did not measure skin surface temperature in our study, studies in humans suggest that immersion of the hand in 12 °C for 5 min results in profound decreases in skin temperature to 15 °C, measured using an infrared skin thermometer immediately after removal of the hand from the water, as measured by an infrared skin thermometer (Traynor and MacDermid, 2008). Thus, it's likely that decreases in Tb were associated with skin temperatures that approximated the water temperature in each condition. In studies using jackets perfused with cold water on rats, the threshold skin temperature to activate BAT sympathetic nerve activity is 37.5 °C (Ootsuka and McAllen, 2006), while the threshold skin temperature to activate tail sympathetic nerve activity is higher, 38.8–40.1 °C (Tanaka et al., 2007). At an ambient temperature of 24 °C, rat tail skin temperature has been measured to be between 26 °C to 27 °C (Sakurada et al., 1993; Cerri et al., 2010). Thus, it is likely that 19 °C and to some extent 25 °C water temperature conditions in our study resulted in activation of these two sympathetic pathways involved in cold defense.

Exposure of rats to a 15 min SS at 19 °C resulted in an increase in immobility. A recent study found no effects of water temperature on immobility during a 5 minute test session of forced swim at 20 °C, 25 °C, or 30 °C, using a water depth of 30 cm, although levels of immobility were decreased during 15 °C swim relative to 30 °C swim (Pinter et al., 2011). Consistent with findings by Pinter and colleagues, Jefferys and Funder (1994) found that rats exposed to 20 °C water during the first 15 minute forced swim exposure had lower levels of immobility compared to rats exposed to either 25 °C or 30 °C water. It's unclear why these previous studies found that cold swim decreases immobility, while our study found that cold swim increases immobility. These discrepancies could be due to methodological differences in the forced swim procedure, or to differences in behavioral coding. During our 15 minute swim stress exposure, rats exposed to 19 °C displayed a

stereotyped behavior wherein the rat would position itself horizontally at the water's surface for extended periods of time, displaying only small forelimb movements for lateral stability; we classified this behavior as immobility in our study. It is plausible that this behavior was not possible for rats in the studies by Pinter and colleagues and by Jefferys and Funder as they used smaller diameter swim tanks (14 cm or 18 cm diameter, respectively, versus 30 cm diameter in our study). The unique behavior observed in rats exposed to 19 °C in our study may be functionally quite different from immobility under other conditions, and is likely to account for the differential effects of cold swim on immobility in our study (increased immobility) and previous studies (decreased immobility). Previous work has shown that water depth affects immobility time on the second day of the forced swim test when performed at either 25 °C or 30 °C; shallower water depths result in increased immobility, in part due to the ability of the rat to support its body with its tail (Abel, 1994; Pinter et al., 2011). It is currently unknown how water depth affects behavior in the first day of the forced swim test. Our studies intentionally used a water depth that prevents the rat from supporting its body with its tail, as recommended by Lucki and colleagues (Detke et al., 1995), and this fundamental difference may have influenced the way the rats coped with the stressor under different temperature conditions.

Regardless of the temperature conditions, SS increased c-Fos expression in serotonergic and non-serotonergic neurons in the multiple subdivisions of the DR. The widespread activation of serotonergic systems in our study is inconsistent with a previous study in which SS (15 min; 25 °C) resulted in regionally specific increases in c-Fos expression in serotonergic neurons in the caudal part of the DR (DRC) and DRI (Commons, 2008). These differences may be due to the fact that in the studies by Commons (2008), quantification of c-Fos expression was conducted using immunofluorescence whereas our studies used immunoperoxidase staining methods, and the sensitivity of these methods for detection of c-Fos may differ.

Swim stress at 19 °C resulted in a greater increase in c-Fos expression in serotonergic neurons, relative to either 25 °C or 35 °C, in the DRVL/VLPAG and DRI. Activation of a small number of serotonergic neurons in the DRVL/VLPAG and DRI regions following SS is consistent with previous studies examining the effects of SS on c-Fos expression within DR serotonergic neurons (Commons, 2008; Roche et al., 2003). Both the DRVL/VLPAG and DRI have been implicated in responses to warm ambient temperature (Hale et al., 2011) and responses to the pyrogen, lipopolysaccharide (Hollis et al., 2006), suggesting that these subregions of the DR may be uniquely thermosensitive. Supporting this hypothesis, local warming of the midbrain results in increased neuronal firing rates within the DRVL/VLPAG and DRI regions (Cronin and Baker, 1977). In our studies, activation of DRVL/VLPAG and DRI serotonergic neurons is likely due to afferent signaling from thermoreceptors in the skin, via a spinoparabrachial pathway that synapses within the LPB (Nakamura and Morrison, 2008; Nakamura and Morrison, 2010). Selective activation of serotonergic neurons in the DRVL/VLPAG and DRI at 19 °C, relative to 25 °C or 35 °C, may be due to selective afferents to these regions from neural circuits controlling thermoregulatory responses, including the LPB and MPO. The LPB gives rise to glutamatergic projections to the DR (Lee et al., 2003). Although a number of subregions of the DR, including the mid-rostrocaudal DRD and DRV, DRVL/VLPAG, and DRC/DRI, appear to receive some afferents from the LPB, it remains possible that a cold-sensitive subpopulation of afferents selectively targets the DRVL/VLPAG and DRI subregions. The anterior hypothalamic/MPO also projects to the DR, and these projections densely innervate the DRVL/VLPAG and DRI regions (Holstege, 1995); therefore, the topographically specific activation of the DRVL/VLPAG and DRI regions by cold temperature exposure could be due to afferents from the LPB, the thermoregulatory component of the MPO, or both.

It seems paradoxical that both warm ambient temperature (Hale et al., 2011) and cold swim, in our study, selectively activated serotonergic neurons in the DRVL/VLPAG and DRI regions. If these are the same serotonergic neurons, then is seems unlikely that they are involved in thermoregulatory responses, as the thermoregulatory requirements are opposite under these conditions. However, it is likely that warm- versus cold-activated serotonergic neurons represent different populations of neurons within the same subregions of the DR. In support of this possibility, studies in anesthetized cats have shown that both cold-sensitive and warm-sensitive neurons can be found in close proximity within the DRVL/VLPAG region (Cronin and Baker, 1977).. Therefore, although exposure to warm and cold stimuli both activate serotonergic neurons in the DRVL/VLPAG and DRI regions, it is possible that these are different populations of neurons. This hypothesis could be tested using currently available mouse models that permit visualization of sequential activation of populations of neurons in the same organism (Reijmers et al., 2007), or chronic recording. The greater increase in c-Fos expression in the DRVL/VLPAG and DRI regions at 19 °C, relative to either 25 °C or 35 °C, could reflect a greater aversiveness of cold temperature exposure, rather than cold temperature *per se*. This seems unlikely, however, as a number of aversive stimuli fail to activate serotonergic neurons in these regions (Lowry et al., 2008; Lowry and Hale, 2010; Hale and Lowry, 2010) and cold swim on the second day of forced swim paradigm, relative to swimming at warmer water temperatures, does not potentiate SS-induced activation of the HPA axis measured immediately after a 5 minute forced swim (Pinter et al., 2011).

A previous study by Linthorst and colleagues (2008) found that, while extracellular 5-HT and 5-HIAA concentrations in the dorsal and ventral fields of the temporal pole of the hippocampus are increased during swim exposure at 35 °C, there was no increase in either extracellular 5-HT or 5-HIAA concentrations during swim exposure in rats tested at 19 °C; in contrast, extracellular 5-HIAA concentrations decreased during swim exposure. These findings seem contradictory to our findings, where cold swim exposure increased c-Fos expression in the DRVL/VLPAG and DRI regions. One potential explanation is that the delayed increases in extracellular serotonin and 5-HIAA concentrations following exposure to SS at 19 °C, which were evident from 45 min to 2 h following the end the 15 min swim session and tightly coupled to the period of thermoregulatory warming, could account for the potentiation of c-Fos expression in the DRVL/VLPAG and DRI regions in our studies. Another potential explanation is that DRVL/VLPAG serotonergic neurons inhibit serotonergic neurons in the DRV or MnR (not included in our analysis) projecting to the ventral hippocampus. This hypothesis is supported by previous studies involving selective lesions of DRVL/VLPAG serotonergic neurons, which resulted in increases in tryptophan hydroxylase mRNA expression selectively in the DRV region (Ljubic-Thibal et al., 1999), which is known to give rise to extensive projections to the ventral hippocampus (Kohler and Steinbusch, 1982; McKenna and Vertes, 2001, Lowry et al., 2008; Lowry and Hale, 2010). While comparing studies using c-Fos immunostaining with studies using microdialysis, it should be noted that a limitation of c-Fos immunohistochemistry is that it is not a viable marker for reductions in cellular activity (e.g. decreases in electrophysiological firing rates; for review see Kovacs, 1998). Moreover, cellular responses can occur independent of c-Fos induction, therefore the absence of c-Fos may not reflect a lack of cellular response to a given treatment (Morgan and Curran, 1989; Chan et al., 1993; Cullinan et al., 1995).

Cold swim stress (19 °C), relative to swim stress at 35 °C, resulted in increased activation of c-Fos in both serotonergic neurons and non-serotonergic cells in the RPa, specifically at −11.60 mm bregma. The RPa contains both serotonergic (Nakamura et al., 2004; Stornetta et al., 2005) and glutamatergic (Nakamura et al., 2002) sympathetic premotor neurons that control cutaneous vasoconstriction and brown adipose tissue thermogenesis. Glutamatergic and serotonergic terminals have been found to synapse onto sympathetic preganglionic

neurons in the intermediolateral column of the spinal cord (Madden and Morrison, 2004). Consistent with these anatomical findings, microinjections of muscimol into the RPa at −11.60 mm reduce stress-induced increases in heart rate and blood pressure (Samuels et al., 2002; Zaretsky et al., 2003) and decrease core body temperature in a home cage environment at an ambient temperature of 24–25 °C (Zaretsky et al., 2003). Confirmation of the neurochemical phenotype of the c-Fos-ir non-serotonergic cells in this region of the RPa in our study will require further studies.

Activation of DRVL/VLPAG and DRI serotonergic neurons was positively correlated with increased c-Fos expression in the LPB, an important part of the thermoafferent signaling pathway from the skin to the central nervous system (Nakamura and Morrison; 2008; Nakamura and Morrison, 2010). Studies by Nakamura and colleagues have shown that exposure of rats to either warm or cold ambient temperature activates glutamatergic neurons in the LPB that project to the MPO (Nakamura and Morrison, 2008; Nakamura and Morrison, 2010), and that cold-sensitive LPB neurons are predominantly located in the LPBel and LPBc subdivisions. Consistent with these findings, we found a greater number of c-Fos-ir cells in the LPBel in rats exposed to 19 °C SS, compared to rats exposed to 35 °C SS. Future studies could examine whether or not inactivation of the LPB is able to block the effects of 19 °C SS-induced activation of DR serotonergic subpopulations.

Activation of DRVL/VLPAG serotonergic neurons was positively correlated with increased c-Fos expression in both serotonergic and non-serotonergic cells within the RPa. The DRVL/VLPAG region projects to the RPa region (Hermann et al., 1997; Bago et al., 2002), and the RPa has been shown by a number of investigators to be part of the efferent thermoregulatory pathways controlling vasoconstriction in cutaneous vascular beds of the tail (Ootsuka et al., 2004), BAT thermogenesis (Morrison et al., 1999; Morrison, 1999; Morrison, 2001) and shivering thermogenesis (Tanaka et al., 2006). Intra-RPa microinjections of glycine or muscimol inhibit BAT thermogenesis (Cao et al., 2004), vasoconstriction in cutaneous vascular beds (Ootsuka and Blessing, 2005) and shivering thermogenesis (Tanaka et al., 2007) in response to thermogenic stimuli. Furthermore, disinhibition of RPa neurons using bicuculline results in increases in interscapular BAT (IBAT) sympathetic nerve activity and IBAT temperature (Morrison, 1999; Morrison, 2001; Morrison et al., 1999). Previous tracing studies have shown that both serotonergic and non-serotonergic neurons in the DRVL/VLPAG project to the MPO (Rizvi et al., 1992; Kanno et al., 2008) and to the RPa (Hermann et al., 1997; Bago et al., 2002). Thus, neurons in the DRVL/VLPAG may either influence RPa activity indirectly via projections to hypothalamic thermoregulatory systems that in turn control RPa function, or directly via projections to RPa.

Activation of DRI serotonergic neurons was correlated with increased c-Fos expression in non-serotonergic cells within the RPa. There is evidence for both serotonergic and non-serotonergic projections from the DRI to the MPO (Tillet, 1992) and therefore DRI serotonergic neurons may also play a role in thermoregulation. Previous studies have characterized expression of 5-HT_{1A} (Marvin et al., 2010) and 5-HT_{1B} (Pazos and Palacios, 1985) receptors in the MPO, and have shown neuromodulatory effects of 5-HT on MPO neurons via 5-HT_{1A} and 5-HT_{1B} receptors (Lee et al., 2008). Superfusion of the 5-HT_{1A} selective agonist, 8-hydroxy-N,N-dipropyl-2-aminotetralin, decreases GABAergic miniature inhibitory postsynaptic current frequencies and superfusion of a 5-HT_{1B} selective agonist, 7-trifluoromethyl-4-(4-methyl-1-piperazinyl)pyrrolo[1,2-a]-quinoxaline dimaleate, decreases miniature excitatory postsynaptic current frequencies (Lee et al., 2008). Previous findings have also shown functional responses to 5-HT in the MPO through intra-MPO injection of 5-HT resulting in either hypothermia (Ruwe and Myers, 1982; Lin et al., 1983) or hyperthermia (Datta et al., 1988; Huttunen et al., 1988). Medial preoptic area responses to 5-

HT may depend on both the specific anatomical coordinates and the administered dose of pharmacological agents. A hypothetical model outlining potential DRI-MPO and DRVL/VLPAG-MPO and/or DRVL/VLPAG-RPa circuits controlling thermoregulatory responses to cold SS is illustrated in Figure 11.

Activation of non-serotonergic neurons in the dorsal raphe nucleus

In the study by Roche and colleagues (2003) investigating the effects of SS on c-Fos expression in serotonergic and non-serotonergic neurons in the DR, about 4% of activated neurons in the DRVL/VLPAG region were serotonergic, and in our study approximately 10% of activated neurons in the DRVL/VLPAG region were found to be serotonergic. Thus, both studies suggest that serotonergic neurons make up only a small percentage of the total population of neurons in the DRVL/VLPAG region that is activated following SS. The neurochemical phenotypes of the SS-sensitive non-serotonergic neurons are unclear, but include γ-aminobutyric acid (GABA)-ergic and glutamatergic neurons (Roche et al., 2003). The function of these non-serotonergic neurons in the DRVL/VLPAG neurons is unclear and will require further investigation.

Conclusions

Our findings are consistent with the hypothesis that subpopulations of serotonergic neurons in the DR (DRVL/VLPAG and DRI subregions) and RPa contribute to thermoregulatory responses to cold temperature. Serotonergic neurons in the DRVL/VLPAG are part of a sympathomotor command system regulating the sympathetic nervous system and motor function (Kerman et al., 2006). Consequently, this population of serotonergic neurons is anatomically well situated to modulate sympathetic and motor function in response to cold ambient temperature. Meanwhile, serotonergic neurons in the DRI project to the MPO and may modulate hypothalamic thermoregulatory systems. However, the fact that serotonergic neurons throughout the DR were activated by SS, independent of ambient temperature, suggests that serotonergic systems are also activated by interoceptive cues related to the aversive nature of the test, and/or in association with the increases in motor activity. For example, DRI serotonergic neurons project to forebrain limbic structures (Lowry et al., 2008) including the hippocampus and medial prefrontal cortex, and therefore may modulate cognitive and affective responses to cold temperature.

Acknowledgments

We gratefully acknowledge the technical assistance of Christopher E. Stamper and Patrick A. Hennessey.

Grants

The work presented was supported by the National Science Foundation through a CAREER Award to CAL; Grant No. 0845550 and by the National Institutes of Health through a RO1 award to CAL; Grant No. 1RO1MH086359-01.. Any opinions, findings, and conclusions or recommendations in this material are those of the authors and do not necessarily reflect the views of the National Science Foundation or the National Institutes of Health.

Abbreviations

5-HT	5-hydroxytryptamine, serotonin
5-HIAA	5-hydroxyindoleacetic acid
5-HT$_{1A}$	serotonin receptor, 1A subtype
5-HT$_{1B}$	serotonin receptor, 1B subtype

5-HT$_{2A}$	serotonin receptor, 2A subtype
8-OH-DPAT	8-hydroxy-N,N-dipropyl-2-aminotetralin
ANOVA	analysis of variance
BAT	brown adipose tissue
DA	dorsal hypothalamic area
DAB	3-3′-diaminobenzidine tetrahydrochloride
DMH	dorsomedial hypothalamus
DR	dorsal raphe nucleus
DRC	dorsal raphe nucleus, caudal part
DRD	dorsal raphe nucleus, dorsal part
DRI	dorsal raphe nucleus, interfascicular part
DRV	dorsal raphe nucleus, ventral part
DRVL/VLPAG	dorsal raphe nucleus, ventrolateral part/ventrolateral periaqueductal gray
GABA	γ-aminobutyric acid HC, home cage
IBAT	intrascapular brown adipose tissue
ir	immunoreactive
LPB	lateral parabrachial nucleus
LPBel	lateral parabrachial nucleus, external lateral part
LPBd	lateral parabrachial nucleus, dorsal part
LSD	least significant difference
MPO	medial preoptic area
MnR	median raphe nucleus
PB	sodium phosphate buffer
PBS	phosphate-buffered saline
PBST	phosphate-buffered saline with 0.1% Triton X-100
RPa	raphe pallidus nucleus
SS	swim stress
Tb	core body temperature
TPH	tryptophan hydroxylase
TPH1	tryptophan hydroxylase 1
TPH2	tryptophan hydroxylase 2
TRP	transient receptor potential
TRPM8	transient receptor potential channel, subfamily M, member 8

References

Abel EL. Behavioral and physiological effects of different water depths in the forced swim test. Physiol Behav. 1994; 56:411–414. [PubMed: 7938258]

Abrams JK, Johnson PL, Hollis JH, Lowry CA. Anatomical and functional topography of the dorsal raphe nucleus. Ann NY Acad Sci. 2004; 1018:46–57. [PubMed: 15240351]

Bago M, Marson L, Dean C. Serotonergic projections to the rostroventrolateral medulla from midbrain and raphe nuclei. Brain Res. 2002; 945:249–258. [PubMed: 12126887]

Bautista DM, Siemens J, Glazer JM, Tsuruda PR, Basbaum AI, Stucky CL, Jordt SE, Julius D. The menthol receptor TRPM8 is the principal detector of environmental cold. Nature. 2007; 448:204–208. [PubMed: 17538622]

Bester H, Chapman V, Besson JM, Bernard JF. Physiological properties of the lamina I spinoparabrachial neurons in the rat. J Neurophysiol. 2000; 83:2239–2259. [PubMed: 10758132]

Bester H, Matsumoto N, Besson JM, Bernard JF. Further evidence for the involvement of the spinoparabrachial pathway in nociceptive processes: a c-Fos study in the rat. J Comp Neurol. 1997; 383:439–458. [PubMed: 9208992]

Bratincsak A, Palkovits M. Activation of brain areas in rat following warm and cold ambient exposure. Neuroscience. 2004; 127:385–397. [PubMed: 15262329]

Bratincsak A, Palkovits M. Evidence that peripheral rather than intracranial thermal signals induce thermoregulation. Neuroscience. 2005; 135:525–532. [PubMed: 16125855]

Cannon B, Nedergaard J. Brown adipose tissue: function and physiological significance. Physiol Rev. 2004; 84:277–359. [PubMed: 14715917]

Cano G, Passerin AM, Schiltz JC, Card JP, Morrison SF, Sved AF. Anatomical substrates for the central control of sympathetic outflow to interscapular adipose tissue during cold exposure. J Comp Neurol. 2003; 460:303–326. [PubMed: 12692852]

Cao WH, Fan W, Morrison SF. Medullary pathways mediating specific sympathetic responses to activation of dorsomedial hypothalamus. Neuroscience. 2004; 126:229–240. [PubMed: 15145088]

Cerri M, Morrison SF. Corticotropin releasing factor increases in brown adipose tissue thermogenesis and heart rate through dorsomedial hypothalamus and medullary raphe pallidus. Neuroscience. 2006; 140:711–721. [PubMed: 16580142]

Cerri M, Zamboni G, Tupone D, Dentico D, Luppi M, Martelli D, Perez E, Amici R. Cutaneous vasodilation elicited by disinhibition of the caudal portion of the rostral ventromedial medulla of the free-behaving rat. Neuroscience. 2010; 165:984–995. [PubMed: 19895871]

Chan RK, Brown ER, Ericsson A, Kovács KJ, Sawchenko PE. A comparison of two immediate-early genes, c-fos and NGFI-B, as markers for functional activation in stress-related neuroendocrine circuitry. J Neurosci. 1993; 13:5126–5138. [PubMed: 8254363]

Chung KK, Martinez M, Herbert J. Central serotonin depletion modulates the behavioural, endocrine and physiological responses to repeated social stress and subsequent c-fos expression in the brains of male rats. Neuroscience. 1999; 92:613–625. [PubMed: 10408610]

Chung KK, Martinez M, Herbert J. C-Fos expression, behavioural, endocrine and autonomic responses to acute social stress in male rats after chronic restraint: modulation by serotonin. Neuroscience. 2000; 95:453–463. [PubMed: 10658625]

Colburn RW, Lubin ML, Stone DJ Jr, Wang Y, Lawrence D, D'Andrea MR, Brandt MR, Liu Y, Flores CM, Qin N. Attenuated cold sensitivity in TRPM8 null mice. Neuron. 2007; 54:379–386. [PubMed: 17481392]

Commons KG. Evidence for topographically organized endogenous 5-HT-1A receptor-dependent feedback inhibition of the ascending serotonin system. Eur J Neurosci. 2008; 27:2611–2618. [PubMed: 18513318]

Cronin MJ, Baker MA. Thermosensitive midbrain neurons in the cat. Brain Res. 1977; 128:461–472. [PubMed: 884494]

Cullinan WE, Herman JP, Battaglia DF, Akil H, Watson SJ. Pattern and time course of immediate early gene expression in rat brain following acute stress. Neuroscience. 1995; 64:477–505. [PubMed: 7700534]

Datta S, Kumar VM, Chhina GS, Singh B. Interrelationship of thermal and sleep-wakefulness changes elicited from the medial preoptic area in rats. Exp Neurol. 1988; 100:40–50. [PubMed: 3350096]

Detke MJ, Rickels M, Lucki I. Active behaviors in the rat forced swimming test differentially produced by serotonergic and noradrenergic antidepressants. Psychopharmacology (Berl). 1995; 121:66–72. [PubMed: 8539342]

Dhaka A, Murray AN, Mathur J, Earley TJ, Petrus MJ, Patapoutian A. TRPM8 is required for cold sensation in mice. Neuron. 2007; 54:371–378. [PubMed: 17481391]

Dib B, Rompre PP, Amir S, Shizgal P. Thermogenesis in brown adipose tissue is activated by electrical stimulation of the rat dorsal raphe nucleus. Brain Res. 1994; 650:149–152. [PubMed: 7953666]

Drugan RC, Eren S, Hazi A, Silva J, Christianson JP, Kent S. Impact of water temperature and stressor controllability on swim stress-induced changes in body temperature, serum corticosterone, and immobility in rats. Pharmacol Biochem Behav. 2005; 82:397–403. [PubMed: 16236352]

Golozoubova V, Cannon B, Nedergaard J. UCP1 is essential for adaptive adrenergic nonshivering thermogenesis. Am J Physiol Endocrinol Metab. 2006; 291:E350–E357. [PubMed: 16595854]

Golozoubova V, Hohtola E, Matthias A, Jacobsson A, Cannon B, Nedergaard J. Only UCP1 can mediate adaptive nonshivering thermogenesis in the cold. FASEB J. 2001; 15:2048–2050. [PubMed: 11511509]

Grubbs FE. Procedures for Detecting Outlying Observations in Samples. Technometrics. 1969; 11:1–21.

Hale MW, Dady KF, Evans AK, Lowry CA. Evidence for *in vivo* thermosensitivity of serotonergic neurons in the rat dorsal raphe nucleus and raphe pallidus nucleus implicated in thermoregulatory cooling. Exp Neurol. 2011; 227:264–278. [PubMed: 21111735]

Hale MW, Lowry CA. Functional topography of midbrain and pontine serotonergic systems: implications for synaptic regulation of serotonergic circuits. Psychopharmacology (Berl). 2010; 213:243–264. [PubMed: 21088958]

Hedlund PB, Sutcliffe JG. Functional, molecular and pharmacological advances in 5-HT7 receptor research. Trends Pharmacol Sci. 2004; 25:481–486. [PubMed: 15559250]

Hermann DM, Luppi PH, Peyron C, Hinckel P, Jouvet M. Afferent projections to the rat nuclei raphe magnus, raphe pallidus and reticularis gigantocellularis pars alpha demonstrated by iontophoretic application of choleratoxin (subunit b). J Chem Neuroanat. 1997; 13:1–21. [PubMed: 9271192]

Hodges MR, Richerson GB. The role of medullary serotonin (5-HT) neurons in respiratory control: contributions to eupneic ventilation, CO2 chemoreception, and thermoregulation. J Appl Physiol. 2010; 108:1425–1432. [PubMed: 20133432]

Hollis JH, Evans AK, Bruce KP, Lightman SL, Lowry CA. Lipopolysaccharide has indomethacin-sensitive actions on Fos expression in topographically organized subpopulations of serotonergic neurons. Brain Behav Immun. 2006; 20:569–577. [PubMed: 16554144]

Holstege, G. The basic, somatic, and emotional components of the motor system in mammals. In: Paxinos, G., editor. The Rat Nervous System. San Diego: Academic Press; 1995. p. 137-154.

Huttunen P, Lapinlampi T, Myers RD. Temperature-related release of serotonin from unrestrained rats' pre-optic area perfused with ethanol. Alcohol. 1988; 5:189–193. [PubMed: 3415763]

Jefferys D, Funder J. The effect of water temperature on immobility in the forced swimming test in rats. Eur J Pharmacol. 1994; 253:91–94. [PubMed: 8013553]

Kanno K, Shima S, Ishida Y, Yamanouchi K. Ipsilateral and contralateral serotonergic projections from dorsal and median raphe nuclei to the forebrain in rats: immunofluorescence quantitative analysis. Neurosci Res. 2008; 61:207–218. [PubMed: 18423675]

Kerman IA, Shabrang C, Taylor L, Akil H, Watson SJ. Relationship of presympathetic-premotor neurons to the serotonergic transmitter system in the rat brainstem. J Comp Neurol. 2006; 499:882–896. [PubMed: 17072838]

Kobayashi A, Osaka T. Involvement of the parabrachial nucleus in thermogenesis induced by environmental cooling in the rat. Pflugers Arch. 2003; 446:760–765. [PubMed: 12838424]

Kohler C, Steinbusch H. Identification of serotonin and non-serotonin-containing neurons of the mid-brain raphe projecting to the entorhinal area and the hippocampal formation. A combined

immunohistochemical and fluorescent retrograde tracing study in the rat brain. Neuroscience. 1982; 7:951–975. [PubMed: 7048127]

Koolhaas JM, De Boer SF, Buwalda B, van RK. Individual variation in coping with stress: a multidimensional approach of ultimate and proximate mechanisms. Brain Behav Evol. 2007; 70:218–226. [PubMed: 17914253]

Kovács KJ. c-Fos as a transcription factor: a stressful (re)view from a functional map. Neurochem Int. 1998; 33:287–297. [PubMed: 9840219]

Lee HS, Kim MA, Valentino RJ, Waterhouse BD. Glutamatergic afferent projections to the dorsal raphe nucleus of the rat. Brain Res. 2003; 963:57–71. [PubMed: 12560111]

Lee JJ, Hahm ET, Lee CH, Cho YW. Serotonergic modulation of GABAergic and glutamatergic synaptic transmission in mechanically isolated rat medial preoptic area neurons. Neuropsychopharmacology. 2008; 33:340–352. [PubMed: 17392733]

Light AR, Sedivec MJ, Casale EJ, Jones SL. Physiological and morphological characteristics of spinal neurons projecting to the parabrachial region of the cat. Somatosens Mot Res. 1993; 10:309–325. [PubMed: 8237218]

Lin MT, Wu JJ, Tsay BL. Serotonergic mechanisms in the hypothalamus mediate thermoregulatory responses in rats. Naunyn Schmiedebergs Arch Pharmacol. 1983; 322:271–278. [PubMed: 6866135]

Linthorst AC, Flachskamm C, Reul JM. Water temperature determines neurochemical and behavioural responses to forced swim stress: An in vivo microdialysis and biotelemetry study in rats. Stress. 2008; 11:88–100. [PubMed: 17853068]

Ljubic-Thibal V, Morin A, Diksic M, Hamel E. Origin of the serotonergic innervation to the rat dorsolateral hypothalamus: retrograde transport of cholera toxin and upregulation of tryptophan hydroxylase mRNA expression following selective nerve terminals lesion. Synapse. 1999; 32:177–186. [PubMed: 10340628]

Lowry, CA.; Evans, AK.; Gasser, PJ.; Hale, MW.; Staub, DR.; Shekhar, A. Topographical organization and chemoarchitecture of the dorsal raphe nucleus and the median raphe nucleus. In: Monti, JM.; Pandi-Perumal, BL.; Jacobs, BL.; Nutt, DL., editors. Serotonin and Sleep: Molecular, Functional and Clinical Aspects. Basel: Birkhauser; 2008. p. 25-68.

Lowry, CA.; Hale, MW. Serotonin and the neurobiology of anxious states. In: Mûller, CP.; Jacobs, BL., editors. Handbook of the Behavioral Neurobiology of Serotonin. Amsterdam: Elsevier; 2010. p. 379-398.

Madden CJ, Morrison SF. Excitatory amino acid receptors in the dorsomedial hypothalamus mediate prostaglandin-evoked thermogenesis in brown adipose tissue. Am J Physiol Regul Integr Comp Physiol. 2004; 286:R320–R325. [PubMed: 14563660]

Marvin E, Scrogin K, Dudas B. Morphology and distribution of neurons expressing serotonin 5-HT1A receptors in the rat hypothalamus and the surrounding diencephalic and telencephalic areas. J Chem Neuroanat. 2010; 39:235–241. [PubMed: 20080175]

McKemy DD, Neuhausser WM, Julius D. Identification of a cold receptor reveals a general role for TRP channels in thermosensation. Nature. 2002; 416:52–58. [PubMed: 11882888]

McKenna JT, Vertes RP. Collateral projections from the median raphe nucleus to the medial septum and hippocampus. Brain Res Bull. 2001; 54:619–630. [PubMed: 11403988]

Mendoza KC, McLane VD, Kim S, Griffin JD. Invitro application of gold nanoprobes in live neurons for phenotypical classification, connectivity assessment, and electrophysiological recording. Brain Res. 2010; 1325:19–27. [PubMed: 20170645]

Morgan JI, Curran T. Stimulus-transcription coupling in neurons: role of cellular immediate-early genes. Trends Neurosci. 1989; 12:459–462. [PubMed: 2479148]

Morrison SF. RVLM and raphe differentially regulate sympathetic outflows to splanchnic and brown adipose tissue. Am J Physiol. 1999; 276:R962–R973. [PubMed: 10198373]

Morrison SF. Differential regulation of brown adipose and splanchnic sympathetic outflows in rat: roles of raphe and rostral ventrolateral medulla neurons. Clin Exp Pharmacol Physiol. 2001; 28:138–143. [PubMed: 11153531]

Morrison SF, Nakamura K. Central neural pathways for thermoregulation. Front Biosci. 2011; 16:74–104. [PubMed: 21196160]

Morrison SF, Sved AF, Passerin AM. GABA-mediated inhibition of raphe pallidus neurons regulates sympathetic outflow to brown adipose tissue. Am J Physiol. 1999; 276:R290–R297. [PubMed: 9950904]

Nakamura K, Matsumura K, Hubschle T, Nakamura Y, Hioki H, Fujiyama F, Boldogkoi Z, Konig M, Thiel HJ, Gerstberger R, Kobayashi S, Kaneko T. Identification of sympathetic premotor neurons in medullary raphe regions mediating fever and other thermoregulatory functions. J Neurosci. 2004; 24:5370–5380. [PubMed: 15190110]

Nakamura K, Matsumura K, Kaneko T, Kobayashi S, Katoh H, Negishi M. The rostral raphe pallidus nucleus mediates pyrogenic transmission from the preoptic area. J Neurosci. 2002; 22:4600–4610. [PubMed: 12040067]

Nakamura K, Morrison SF. A thermosensory pathway that controls body temperature. Nat Neurosci. 2008; 11:62–71. [PubMed: 18084288]

Nakamura K, Morrison SF. A thermosensory pathway mediating heat-defense responses. Proc Natl Acad Sci U S A. 2010; 107:8848–8853. [PubMed: 20421477]

Nakamura Y, Nakamura K, Matsumura K, Kobayashi S, Kaneko T, Morrison SF. Direct pyrogenic input from prostaglandin EP3 receptor-expressing preoptic neurons to the dorsomedial hypothalamus. Eur J Neurosci. 2005b; 22:3137–3146. [PubMed: 16367780]

Nason MW Jr, Mason P. Modulation of sympathetic and somatomotor function by the ventromedial medulla. J Neurophysiol. 2004; 92:510–522. [PubMed: 14973310]

Nason MW Jr, Mason P. Medullary raphe neurons facilitate brown adipose tissue activation. J Neurosci. 2006; 26:1190–1198. [PubMed: 16436606]

Ootsuka Y, Blessing WW. Activation of slowly conducting medullary raphe-spinal neurons, including serotonergic neurons, increases cutaneous sympathetic vasomotor discharge in rabbit. Am J Physiol Regul Integr Comp Physiol. 2005; 288:R909–R918. [PubMed: 15550616]

Ootsuka Y, Blessing WW, McAllen RM. Inhibition of rostral medullary raphe neurons prevents cold-induced activity in sympathetic nerves to rat tail and rabbit ear arteries. Neurosci Lett. 2004; 357:58–62. [PubMed: 15036613]

Ootsuka Y, McAllen RM. Comparison between two rat sympathetic pathways activated in cold defense. Am J Physiol Regul Integr Comp Physiol. 2006; 291:R589–R595. [PubMed: 16601257]

Paxinos, G.; Watson, C. The Rat Brain in Stereotaxic Coordinates. 4. San Diego: Academic Press; 1998.

Pazos A, Palacios JM. Quantitative autoradiographic mapping of serotonin receptors in the rat brain. I. Serotonin-1 receptors. Brain Res. 1985; 346:205–230. [PubMed: 4052776]

Peier AM, Moqrich A, Hergarden AC, Reeve AJ, Andersson DA, Story GM, Earley TJ, Dragoni I, McIntyre P, Bevan S, Patapoutian A. A TRP channel that senses cold stimuli and menthol. Cell. 2002; 108:705–715. [PubMed: 11893340]

Petersen, RG. Design and Analysis of Experiments. New York: Marcel Dekker, Inc; 1985.

Pinter O, Domokos A, Mergl Z, Mikics E, Zelena D. Do stress hormones connect environmental effects with behavior in the forced swim test? Endocr J. 2011; 58:395–407. [PubMed: 21505269]

Rathner JA, McAllen RM. The lumbar preganglionic sympathetic supply to rat tail and hindpaw. J Auton Nerv Syst. 1998; 69:127–131. [PubMed: 9696268]

Ray RS, Corcoran AE, Burst RD, Kim JC, Richerson GB, Nattie E, Dymeck SM. Impaired respiratory and body temperature control upon acute serotonergic neuron inhibition. Science. 2011; 33:637–642. [PubMed: 21798952]

Reijmers LG, Perkins BL, Matsuo N, Mayford M. Localization of a stable neural correlate of associative memory. Science. 2007; 317:1230–1233. [PubMed: 17761885]

Rinaman L, Stricker EM, Hoffman GE, Verbalis JG. Central c-Fos expression in neonatal and adult rats after subcutaneous injection of hypertonic saline. Neuroscience. 1997; 79:1165–1175. [PubMed: 9219975]

Rizvi TA, Ennis M, Shipley MT. Reciprocal connections between the medial preoptic area and the midbrain periaqueductal gray in rat: a WGA-HRP and PHA-L study. J Comp Neurol. 1992; 315:1–15. [PubMed: 1371779]

Roche M, Commons KG, Peoples A, Valentino RJ. Circuitry underlying regulation of the serotonergic system by swim stress. J Neurosci. 2003; 23:970–977. [PubMed: 12574426]

Ruwe WD, Myers RD. 5-HT receptors and hyper- or hypothermia: elucidation by catecholamine antagonists injected into the cat hypothalamus. Brain Res Bull. 1982; 8:79–86. [PubMed: 7055736]

Sakurada S, Shido O, Fujikake K, Nagasaka T. Relationship between body core and peripheral temperatures at the onset of thermoregulatory responses in rats. Jpn J Physiol. 1993; 43:659–667. [PubMed: 8145403]

Samuels BC, Zaretsky DV, DiMicco JA. Tachycardia evoked by disinhibition of the dorsomedial hypothalamus in rats is mediated through medullary raphe. J Physiol. 2002; 538:941–6. [PubMed: 11826177]

Stornetta RL, Rosin DL, Simmons JR, McQuiston TJ, Vujovic N, Weston MC, Guyenet PG. Coexpression of vesicular glutamate transporter-3 and gamma-aminobutyric acidergic markers in rat rostral medullary raphe and intermediolateral cell column. J Comp Neurol. 2005; 492:477–494. [PubMed: 16228993]

Tanaka M, Ootsuka Y, McKinley MJ, McAllen RM. Independent vasomotor control of rat tail and proximal hairy skin. J Physiol. 2007; 582:421–433. [PubMed: 17430987]

Tanaka M, Owens NC, Nagashima K, Kanosue K, McAllen RM. Reflex activation of rat fusimotor neurons by body surface cooling, and its dependence on the medullary raphe. J Physiol. 2006; 572:569–583. [PubMed: 16484305]

Tillet Y. Serotoninergic projections from the raphe nuclei to the preoptic area in sheep as revealed by immunohistochemistry and retrograde labeling. J Comp Neurol. 1992; 320:267–272. [PubMed: 1619053]

Traynor R, MacDermid JC. Immersion in Cold-Water Evaluation (ICE) and self-reported cold intolerance are reliable but unrelated measures. Hand (N Y). 2008; 3:212–219. [PubMed: 18780098]

Yoshida K, Li X, Cano G, Lazarus M, Saper CB. Parallel preoptic pathways for thermoregulation. J Neurosci. 2009; 29:11954–11964. [PubMed: 19776281]

Zaretsky DV, Zaretskaia MV, Samuels BC, Cluxton LK, DiMicco JA. Microinjection of muscimol into raphe pallidus suppresses tachycardia associated with air stress in conscious rats. J Physiol. 2003; 546:243–50. [PubMed: 12509492]

Zaretsky DV, Zaretskaia MV, DiMicco JA. Stimulation and blockade of GABA(A) receptors in the raphe pallidus: effects on body temperature, heart rate, and blood pressure in conscious rats. Am J Physiol Regul Integr Comp Physiol. 2003; 285:R110–R116. [PubMed: 12609814]

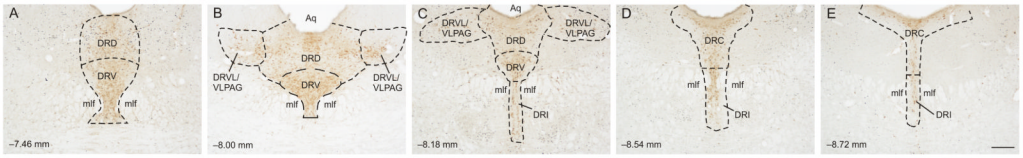

Figure 1.

Low magnification photomicrographs illustrating c-Fos and tryptophan hydroxylase (TPH) immunostaining from different rostrocaudal levels of the dorsal raphe nucleus (DR). c-Fos immunostaining can be identified by a dark blue/black nuclear stain. Tryptophan hydroxylase-immunoreactive (ir) neurons and dendrites can be identified by a red/brown stain. The rostrocaudal levels selected for analysis were A) −7.46 mm bregma, B) −8.00 mm bregma, C) −8.18 mm bregma, D) −8.54 mm bregma, and E) −8.72 mm bregma. The subdivisions of the DR that were analyzed at each rostrocaudal level are delineated by dashed lines. Abbreviations: Aq, cerebral aqueduct; DRC, dorsal raphe nucleus, caudal part; DRD, dorsal raphe nucleus, dorsal part; DRI, dorsal raphe nucleus, interfascicular part; DRV, dorsal raphe nucleus, ventral part; DRVL/VLPAG, dorsal raphe nucleus, ventrolateral part/ventrolateral periaqueductal gray; mlf, medial longitudinal fasciculus. Scale bar, 250 μm.

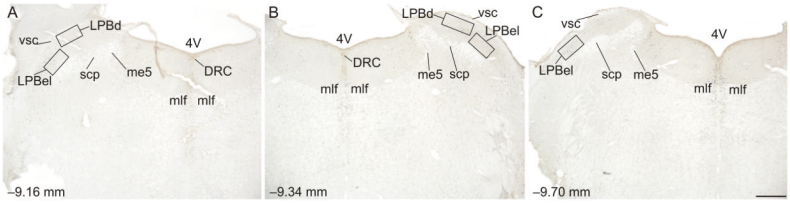

Figure 2.

Low magnification photomicrographs illustrating c-Fos and tryptophan hydroxylase (TPH) immunostaining from different rostrocaudal levels of the medulla containing the lateral parabrachial nucleus (LPB). C-Fos immunostaining can be identified by a dark blue/black nuclear stain. Tryptophan hydroxylase-immunoreactive (ir) neurons and dendrites in the dorsal raphe nucleus, caudal part (DRC) can be identified by a red/brown stain. The rostrocaudal levels selected for analysis were A) −9.16 mm bregma, B) − 9.34 mm bregma, and C) −9.70 mm bregma; black boxes indicate regions selected for analysis. The external lateral part of the LPB (LPBel) was analyzed using a 0.4 × 0.2 mm grid at each rostrocaudal level. The dorsal subdivision of the LPB (LPBd) was analyzed using a 0.4 × 0.2 mm grid at −9.16 mm bregma and a 0.5 × 0.2 mm grid at −9.34 mm bregma. Abbreviations: 4V, 4th ventricle; LPBd, lateral parabrachial nucleus, dorsal part; LPBel, lateral parabrachial nucleus, external lateral part; mlf, medial longitudinal fasciculus; me5, mesencephalic trigeminal tract; scp, superior cerebellar peduncle; vsc, ventral spinocerebellar tract. Scale bar, 500 μm.

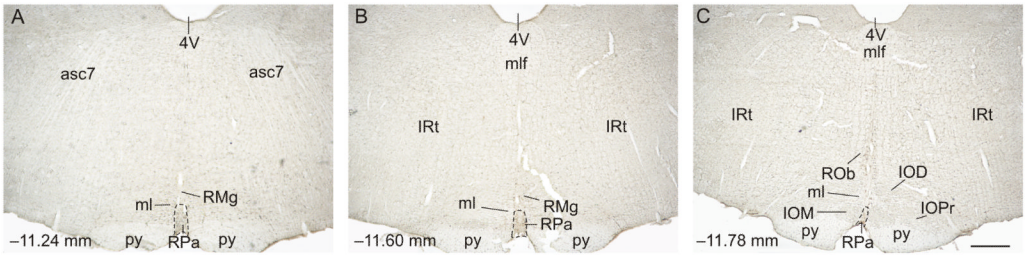

Figure 3.

Low magnification photomicrographs illustrating c-Fos and tryptophan hydroxylase (TPH) immunostaining from different rostrocaudal levels of the medullary raphe nuclei. c-Fos immunostaining can be identified by a dark blue/black nuclear stain. Tryptophan hydroxylase-immunoreactive (ir) neurons and dendrites can be identified by a red/brown stain. The rostrocaudal levels selected for analysis were A) −11.24 mm bregma, B) −11.60 mm bregma, and C) −11.78 mm bregma. The raphe pallidus nucleus (RPa) was analyzed at all three levels. Abbreviations: 4V, 4th ventricle; asc7, ascending fibers of the facial nerve; IOD, inferior olive, dorsal nucleus; IOM, inferior olive, medial nucleus; IRt, intermediate reticular nucleus; ml, medial lemniscus; py, pyramidal tract; RMg, raphe magnus nucleus; RPa, raphe pallidus nucleus; ROb, raphe obscurus nucleus. Scale bar, 500 μm.

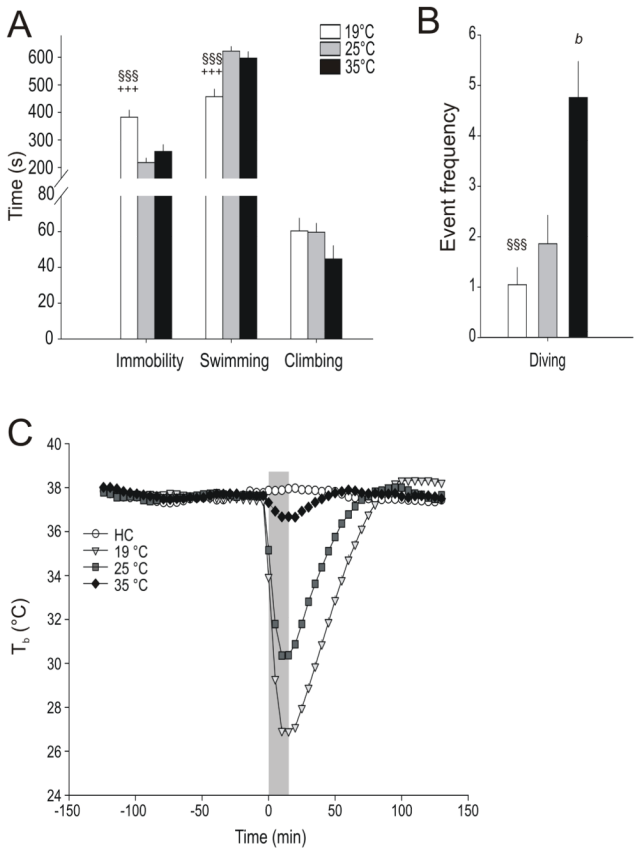

Figure 4.

Graphs illustrating the effects of 19 °C, 25 °C, and 35 °C water temperature on 15 minute swim stress (SS) test behaviors and body temperature (Tb). A) Graph illustrating behaviors scored continuously during SS including: immobility, swimming, and climbing behaviors (see methods for descriptions of behaviors); graph displays mean total time + SEM; +++p < 0.001 vs 25 °C, §§§p < 0.001 vs 35 °C; post hoc Fisher's Protected Least Significant Difference (LSD) test. B) Graph illustrating the frequency of diving behavior during SS (see methods for description of behavior); graph displays mean event frequency + SEM; §§§p < 0.001 vs 35 °C; bp < 0.01 vs 25 °C, post hoc Fisher's Protected Least Significant Difference (LSD) test (19 °C, n = 9; 25 °C, n = 9; 35 °C, n= 9). C) Line and scatterplot graph displaying the effects of home cage (HC, n = 8) conditions, or a 15 minute swim stress (SS) with varying water temperatures (19 °C, n = 9; 25 °C, n = 9; 35 °C, n= 9) on core body temperature measured using a biotelemetry probe. Core body temperature was sampled for 5 sec every minute; data represent mean Tb ± SEM during 5 min periods. Grey bar indicates the 15 minute SS period. Home cage rats were left undisturbed during the 15 minute SS.

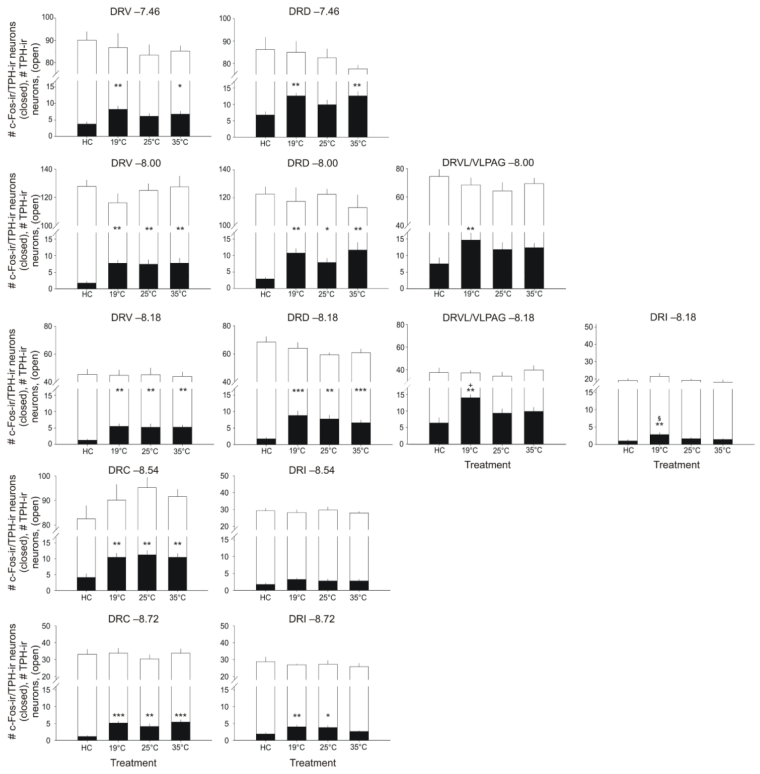

Figure 5.

Graphs illustrating the effects of swim stress at different water temperatures on the numbers of c-Fos-immunoreactive (ir)/tryptophan hydroxylase (TPH)-ir neurons compared with home cage control (HC) conditions within different subdivisions of the dorsal raphe nucleus (DR). Open bars represent mean (+ SEM) values for the total numbers of TPH-ir neurons sampled., closed bars represent mean values for numbers of c-Fos-ir/TPH-ir neurons; anatomical levels are expressed above each graph as distance from bregma in millimeters. $*p < 0.05$ vs HC, $**p < 0.01$ vs HC, $***p < 0.001$ vs HC; $^{+}p < 0.05$ vs 25 °C, $^{\S}p < 0.05$ vs 35 °C; post hoc Fisher's Protected Least Significant Difference (LSD) test (HC, n = 8; 19 °C, n = 9; 25 °C, n = 9; 35 °C, n = 9). Abbreviations: DRC, dorsal raphe nucleus, caudal part; DRD, dorsal raphe nucleus, dorsal part; DRI, dorsal raphe nucleus, interfascicular part; DRV, dorsal raphe nucleus, ventral part; DRVL/VLPAG, dorsal raphe nucleus, ventrolateral part/ventrolateral periaqueductal gray.

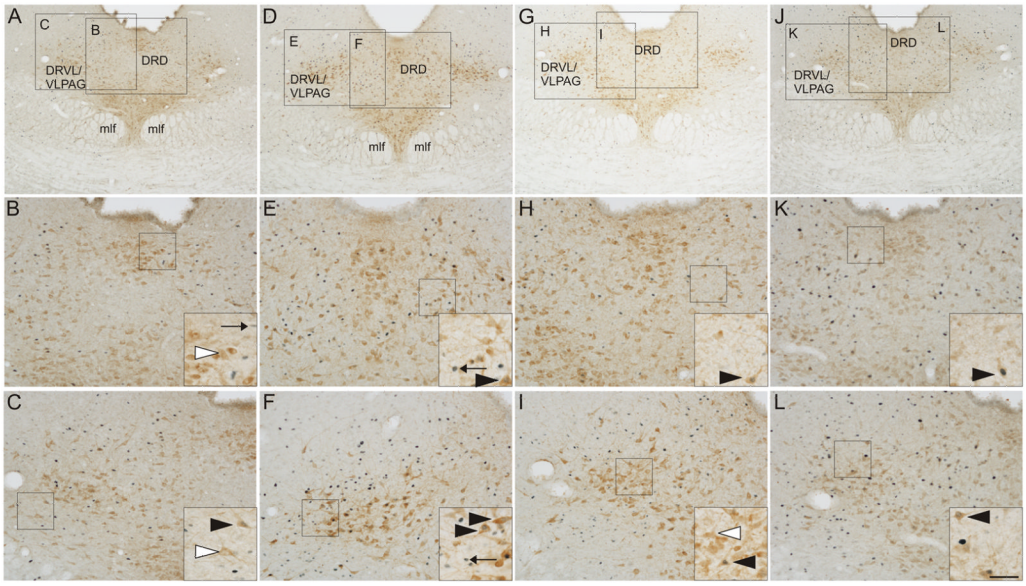

Figure 6.

Photomicrographs illustrate c-Fos/tryptophan hydroxylase (TPH) immunostaining in the mid-rostrocaudal dorsal raphe nucleus (DR; −8.00 mm bregma) in representative rats from each treatment group. Photomicrographs illustrate immunostaining in rats exposed to (A-C) home cage conditions, (D–F) 19 °C swim stress (SS), (G–I) 25 °C SS, and (J–L) 35 °C SS. Black boxes in A, D, G, and J represent regions displayed at higher magnification in B, C, E, F, H, I, K, and L. Black boxes in B, C, E, F, H, I, K, and L indicate regions shown at higher magnification within insets located in the lower right-hand corner of these respective panels. Black arrows indicate representative examples of c-Fos-immunoreactive non-serotonergic cells (blue/black nuclear staining); white arrowheads indicate representative examples of TPH-immunoreactive/c-Fos-immunonegative neurons (red/brown) cytoplasmic staining); black arrowheads indicate representative examples of c-Fos-immunoreactive/TPH-immunoreactive neurons (red/brown) cytoplasmic staining with blue/black nuclear staining). Abbreviations: DRD, dorsal raphe nucleus, dorsal part; DRVL/VLPAG, dorsal raphe nucleus, ventrolateral part/ventrolateral periaqueductal gray; mlf, medial longitudinal fasciculus. Scale bar, 250 μm (A, D, G, J); 100 μm (B, C, E, F, H, I, K, L); 50 μm (insets).

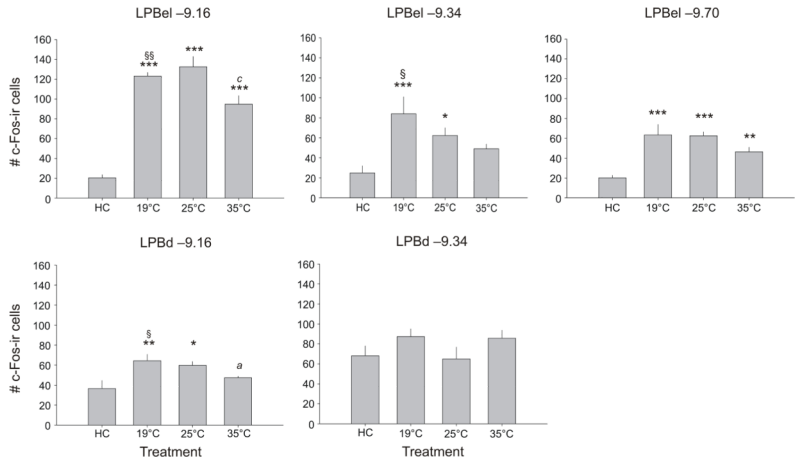

Figure 7.

Graphs illustrating the effect of swim stress at different water temperatures, compared with home cage control (HC) conditions, on the numbers of c-Fos-ir cells (mean + SEM) within different subdivisions of the lateral parabrachial nucleus (LPB). *$p < 0.05$ vs HC, **$p < 0.01$ vs HC, ***$p < 0.001$ vs HC, $^{a}p < 0.05$ vs 25 °C, $^{c}p < 0.001$ vs 25 °C, $^{\S}p < 0.05$ vs 35 °C, $^{\S\S}p < 0.01$ vs 35 °C; post hoc Fisher's Protected Least Significant Difference (LSD) test (HC, n = 8; 19 °C, n = 9; 25 °C, n = 9; 35 °C, n = 9). Anatomical levels are indicated above each graph as distance from bregma in millimeters. Abbreviations: LPBd, lateral parabrachial nucleus, dorsal part; LPBel, lateral parabrachial nucleus, external lateral part.

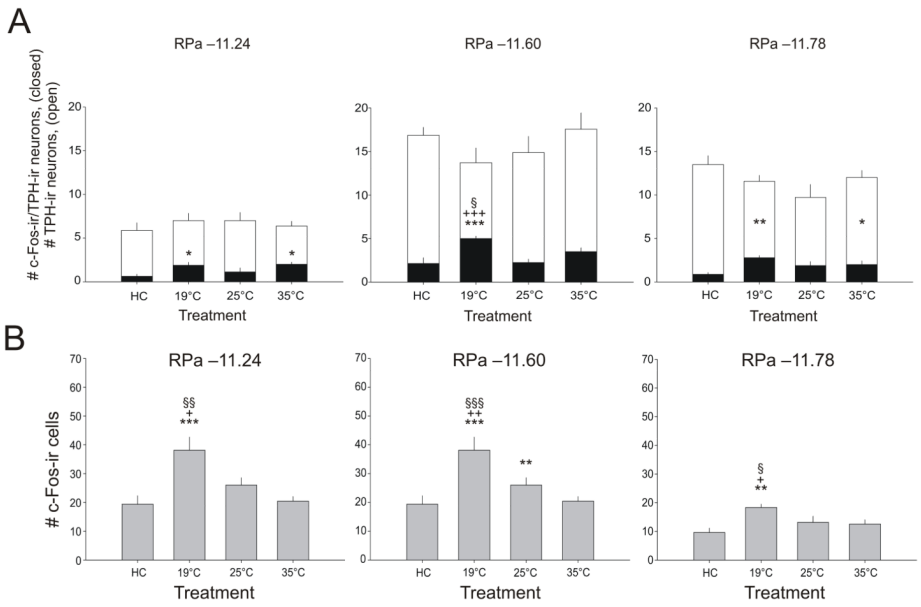

Figure 8.

Graphs illustrating the effects of swim stress at different water temperatures on c-Fos-immunoreactive (ir) serotonergic and non-serotonergic cells in the raphe pallidus nucleus (RPa). A) Graphs illustrating the effect of swim stress at different water temperatures on the numbers of c- Fos-ir/TPH-ir cells (mean + SEM), compared with home cage control (HC) conditions, within different levels of the raphe pallidus nucleus (RPa) HC, n = 8; 19 °C, n = 9; 25 °C, n = 9; 35 °C, n = 9). Open bars represent mean (+ SEM) values for the total numbers of TPH-ir neurons sampled, closed bars represent mean values for numbers of c-Fos-ir/TPH-ir neurons + SEM; anatomical levels are indicated above each graph as distance from bregma in millimeters. B) Graphs illustrating the effect of swim stress at different water temperatures on the numbers of c- Fos-ir/TPH-immunonegative cells (mean + SEM) compared with home cage control (HC) conditions within different levels of the raphe pallidus nucleus (RPa). *$p < 0.05$ vs HC, **$p < 0.01$ vs HC, ***$p < 0.001$ vs HC, + $p < 0.05$ vs 25 °C, ++ $p < 0.01$ vs 25 °C, +++$p < 0.001$ vs 25 °C, § $p < 0.05$ vs 35 °C; post hoc Fisher's Protected Least Significant Difference (LSD) test (HC, n = 8; 19 °C, n = 9; 25 °C, n = 9; 35 °C, n = 9). Anatomical levels are indicated above each graph as distance from bregma in millimeters.

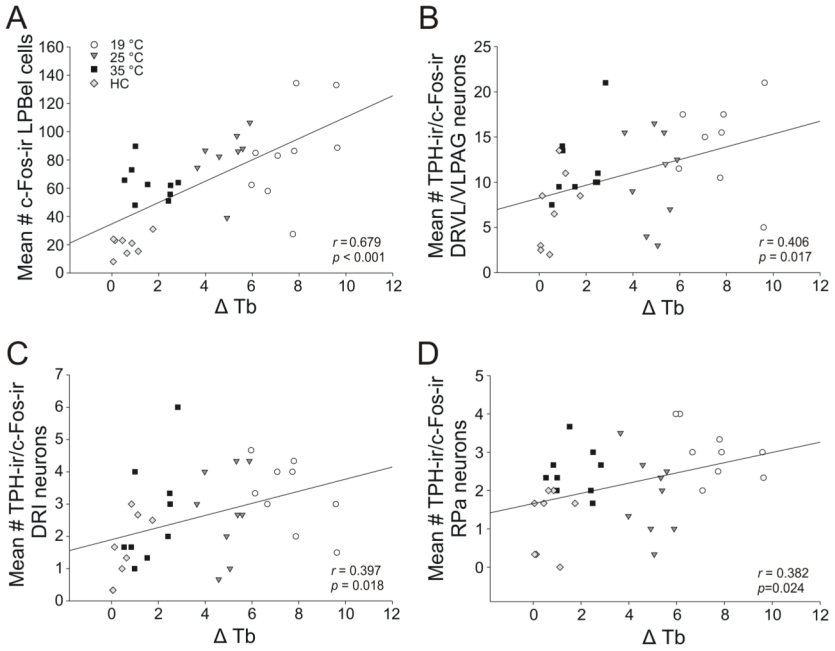

Figure 9.

Scatterplots illustrating correlations between average temperature change from baseline during swim stress (SS; ΔTb) and c-Fos-ir or c-Fos-ir/tryptophan hydroxylase (TPH)-ir neurons in putative spinoparabrachial-raphe circuits. A) Scatterplots illustrating correlations between ΔTb and the average number of c-Fos-ir cells in the lateral parabrachial nucleus, external lateral part (LPBel). Additional scatterplots illustrate correlations between ΔTb and the average number of c-Fos-ir serotonergic neurons in the B) dorsal raphe nucleus, ventrolateral part/ventrolateral periaqueductal gray (DRVL/VLPAG), C) dorsal raphe nucleus, interfascicular part (DRI), and D) raphe pallidus nucleus (RPa).

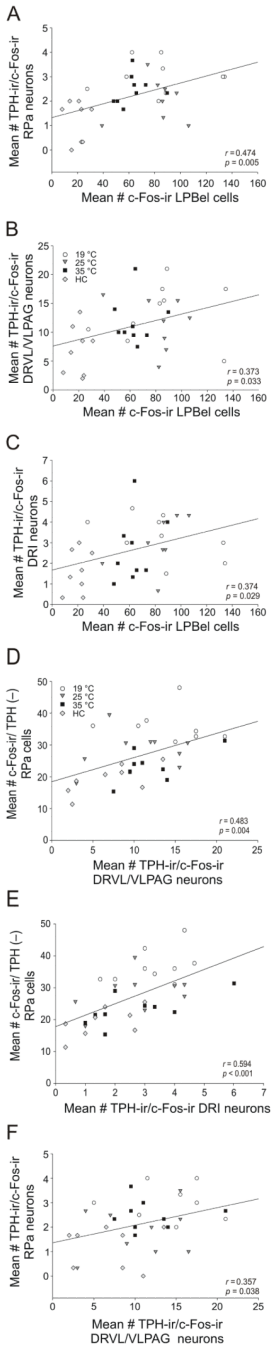

Figure 10.

Scatterplots illustrating correlations among numbers of c-Fos-ir cells in the lateral parabrachial nucleus, external lateral part (LPBel) and c-Fos expression in serotonergic neurons in subdivisions of the dorsal raphe nucleus (DR) and raphe pallidus nucleus (RPa). A-C) Scatterplots illustrate correlations between the average number of c-Fos-ir cells in the lateral parabrachial nucleus and A) RPa, B) the average number of c-Fos-ir/TPH-ir neurons in the dorsal raphe nucleus, ventrolateral part/ventrolateral periaqueductal gray (DRVL/VLPAG), and C) the average number of c-Fos-ir/TPH-ir neurons in the dorsal raphe nucleus, interfasicular part (DRI). D-F) Scatterplots illustrating correlations between numbers of c-Fos-positive serotonergic neurons in subdivisions of the dorsal raphe nucleus

(DR) and numbers of c-Fos-positive serotonergic or non- serotonergic neurons in the raphe pallidus nucleus (RPa). Scatterplots illustrate correlations between D) average number of c-Fos-ir/TPH-ir neurons in the DRVL/VLPAG and average number of c-Fos-ir nonserotonergic cells in the RPa, E) average number of c-Fos-ir/TPH-ir neurons in the dorsal raphe nucleus, interfascicular part (DRI) and the average number of c-Fos-ir nonserotonergic cells in the RPa, and F) average number of c-Fos-ir/TPH-ir neurons in the DRVL/VLPAG and average number of c-Fos-ir/TPH-ir serotonergic neurons in the RPa.

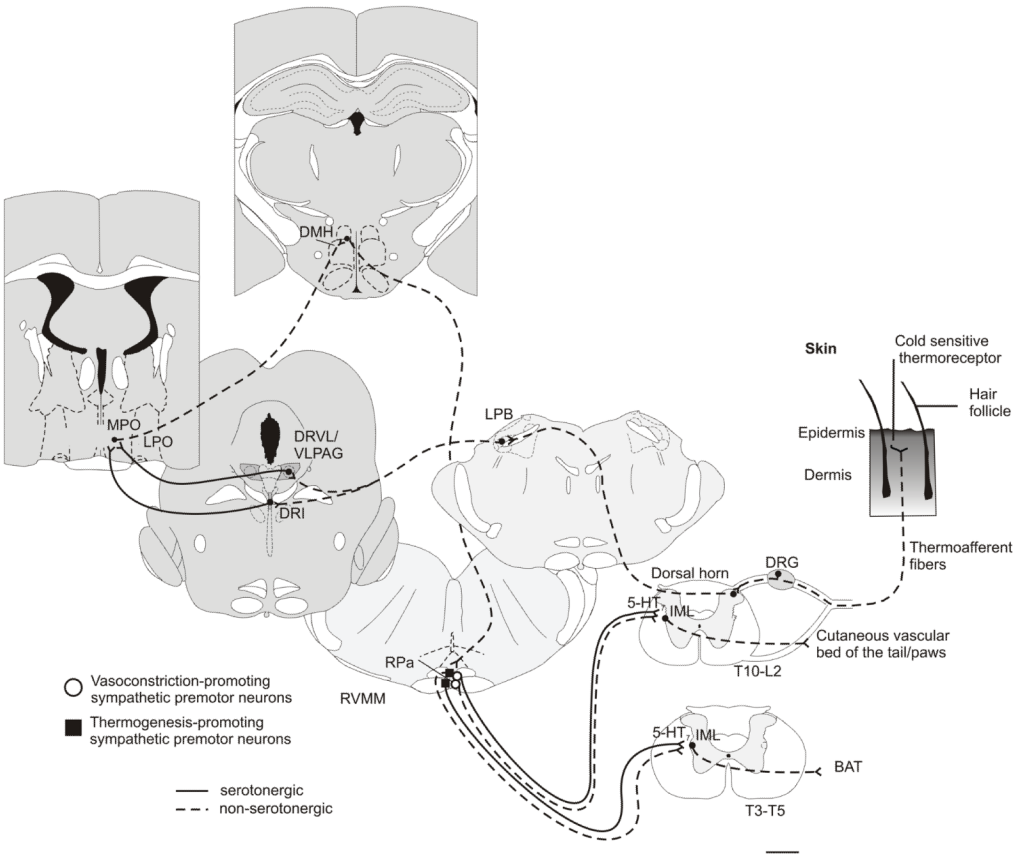

Figure 11.

Hypothetical model illustrating cold-sensitive serotonergic systems. Cold-sensitive transient receptor potential (TRP) channels, specifically transient receptor potential subfamily M member 8 (TRPM8), are necessary for relay of cold temperature information from the periphery to the central nervous system (Dhaka et al., 2007; Colburn et al., 2007; Bautista et al., 2007). TRPM8 is located on free nerve endings of somatosensory neurons whose cell bodies are located in the dorsal root ganglia (Peier et al., 2002; McKemy et al., 2002). It is likely that cold-sensitive ascending ipsilateral and contralateral (Light et al., 1993; Bester et al., 2000) fibers from the dorsal horn to the lateral parabrachial nucleus (LPB), specifically the central and external lateral parts, are glutamatergic (Nakamura and Morrison, 2008). The LPB sends glutamatergic projections to the dorsal raphe nucleus (DR) (Lee et al., 2003). Both the ventrolateral part of the dorsal raphe nucleus/ventrolateral periaqueductal gray (DRVL/VLPAG) (Rizvi et al., 1992; Kano et al., 2008) and the dorsal raphe nucleus, interfascicular part (DRI) (Tillet, 1992) send serotonergic projections to forebrain thermoregulatory areas including the medial preoptic area. GABAergic and glutamatergic projection neurons in the MPO are thought to control dorsomedial hypothalamus/dorsal hypothalamic (DMH/DA) neurons (Nakamura et al., 2005b; Cerri and Morrison, 2006) that in turn project to the raphe pallidus nucleus (RPa) (Yoshida et al., 2009). Previous work has provided evidence that MPO neurons (likely GABAergic) innervate glutamatergic neurons within the DMH that project to the RPa (Nakamura et al., 2005b). Alternatively, there is evidence for glutamatergic projection neurons from the POA to DMH (Mendoza et al., 2010). The RPa contains glutamatergic (Nakamura et al., 2002) and serotonergic (Nakamura et al., 2004; Stornetta et al., 2005) sympathetic premotor neurons that control cutaneous vasoconstriction and brown adipose tissue thermogenesis. Glutamatergic and serotonergic

terminals have been found to synapse onto sympathetic preganglionic neurons in the intermediolateral column of the spinal cord (Madden and Morrison, 2004).

Table 1

Effects of swim stress at different water temperatures, compared with home cage control conditions, on the numbers of c-Fos-ir cells

		c-Fos-ir/TPH-immunonegative			
Region	**Rostrocaudal Level (mm bregma)**	**HC**	**19 °C**	**25 °C**	**35 °C**
DRV	−7.46	38.9 ± 5.39	77.6 ± 5.55$^{***, +, §}$	62.5 ± 5.77**	59.9 ± 3.05**
DRD	−7.46	59.7 ± 4.64	114.6 ± 7.13***	98.6 ± 8.74**	98.7 ± 6.64***
DRV	−8.00	21.0 ± 3.72	63.1 ± 5.84***	47.4 ± 3.90**	60.4 ± 8.64***
DRD	−8.00	49.3 ± 5.82	100.8 ± 7.20***	86.3 ± 9.72**	99.6 ± 6.82***
DRVL/VLPAG	−8.00	75.9 ± 4.23	114.9 ± 2.75$^{***, +}$	96.3 ± 8.84*	112.2 ± 5.32***
DRV	−8.18	12.5 ± 2.15	43.2 ± 3.17$^{***, ++}$	28.0 ± 3.68**	38.5 ± 2.85$^{***, a}$
DRD	−8.18	21.0 ± 3.02	65.5 ± 3.59**	57.8 ± 8.51***	58.4 ± 5.91***
DRVL/VLPAG	−8.18	57.9 ± 3.60	130.8 ± 7.88$^{***, ++, §}$	98.4 ± 8.59***	110.0 ± 6.36***
DRI	−8.18	5.3 ± 1.19	16.9 ± 2.34$^{***, ++, §§}$	11.2 ± 1.18**	9.7 ± 0.57*
DRC	−8.54	29.9 ± 2.55	80.6 ± 6.05***	74.4 ± 6.47***	82.2 ± 4.79***
DRI	−8.54	11.8 ± 1.80	21.6 ± 1.14***	18.1 ± 0.89**	19.0 ± 1.83**
DRC	−8.72	16.5 ± 1.44	31.9 ± 3.39***	26.6 ± 3.46*	27.6 ± 1.50**
DRI	−8.72	11.8 ± 0.96	23.1 ± 1.42$^{***, §}$	24.6 ± 2.52*	17.3 ± 0.80$^{**, b}$

$^{*}p < 0.05$ vs HC,

$^{**}p < 0.01$ vs HC,

$^{***}p < 0.001$ vs HC,

$^{+}p < 0.05$ vs 25 °C,

$^{++}p < 0.01$ vs 25 °C,

$^{a}p<0.05$ vs 25 °C,

$^{b}p <0.01$ vs 25 °C,

$^{§}p < 0.05$ vs 35 °C,

§§ $p < 0.01$ vs 35 °C, post hoc Fisher's Protected Least Significant Difference (LSD) test